TAMPEREEN TEKNILLINEN YLIOPISTO
TAMPERE UNIVERSITY OF TECHNOLOGY

SAARA OSTAMO

DETERMINATION OF VISCOSITY FOR AQUEOUS GELS USING RAMAN SPECTROSCOPY AND MULTIVARIATE ANALYSIS

Master's Thesis

Examiner: professor Helge Lemmetyinen
Examiner and thesis subject approved by the Faculty of Natural Sciences on May 6th 2015

ABSTRACT

SAARA OSTAMO: Determination of viscosity for aqueous gels using Raman spectroscopy and multivariate analysis
Tampere University of Technology
Master of Science Thesis, 46 pages, 11 Appendix pages
August 2015
Master's Degree Programme in Energy and Environmental Technology
Major: Chemistry
Examiner: Professor Helge Lemmetyinen

Keywords: hydrogel, viscosity, Raman spectroscopy, multivariate analysis, PLS regression

This thesis was conducted for Orion Corporation. The aim of this thesis was to examine, whether the viscosity of aqueous gels can be modelled from their Raman spectra with multivariate analysis. Previously the method's applicability for viscosity modelling of mineral oils and kerosene, for example, has been studied and the method's suitability for concentration modelling has been established. In a previous study done for Orion Corporation the suitability of the method for viscosity modelling of gels was discovered. The main objectives of this thesis were to confirm the results of the previous study and to discover the factors affecting the applicability of the method on different materials.

Seven gelling agents used in pharmaceutical industry were examined: potato starch, hydroxyethylcellulose, hydroxypropylcellulose, two carbomers, polyvinylpyrrolidone and a blend containing polyacrylamide. Sample sets were prepared from the gelling agents and water and their viscosities were measured with a rotational rheometer. Four of the materials were suitable for Raman measurements with the selected instrumentation. The Raman spectra of hydroxypropylcellulose, the two carbomers, and polyvinylpyrrolidone, were recorded. Partial Least Squares regression (PLSR) models used for predicting viscosities of unknown samples were constructed based on the Raman spectra.

The carbomers were well suitable for viscosity modelling, and their PLSR models predicted the viscosities of unknown samples accurately. The PLSR model of hydroxypropylcellulose resulted in great variation in the predicted viscosity values, and the model could not be considered reliable. A PLSR model could not be constructed from polyvinylpyrrolidone and therefore its viscosity values could not be predicted.

It was confirmed in this study that the Raman spectroscopic method combined with multivariate analysis can be used for modelling of the viscosity of aqueous gels. No direct causal connection could be established between the material properties and modelling results, however. The most important factors affecting the applicability of the method were the appearance and concentrations of the gels samples. In the future, more comprehensive sample sets with lesser variation between the samples should be studied. More complex materials and the effect of measuring systems of Raman spectra and viscosity should be studied.

TIIVISTELMÄ

SAARA OSTAMO: Vesipohjaisten geelien viskositeetin määrittäminen Raman-spektroskopian ja monimuuttuja-analyysin avulla
Tampereen teknillinen yliopisto
Diplomityö, 46 sivua, 11 liitesivua
Elokuu 2015
Ympäristö- ja energiatekniikan diplomi-insinöörin tutkinto-ohjelma
Pääaine: Kemia
Tarkastaja: professori Helge Lemmetyinen

Avainsanat: hydrogeeli, viskositeetti, Raman-spektroskopia, monimuuttuja-analyysi, PLS-regressio

Tämä diplomityö toteutettiin Orion Oyj:n Turun toimipisteessä. Diplomityössä tutkittiin, voiko vesipohjaisten geelien viskositeettia mallintaa niiden Raman-spektreistä monimuuttuja-analyysin avulla. Aiemmin on tutkittu menetelmän soveltuvuutta esimerkiksi mineraaliöljyjen ja kerosiinin viskositeetin mallinnukseen sekä todettu menetelmän soveltuvan hyvin konsentraation mallintamiseen. Orion Oyj:lle aiemmin laaditussa diplomityössä havaittiin menetelmän mahdollinen soveltuvuus myös geelien viskositeetin mallinnukseen. Tämän työn tärkeimpinä tavoitteina oli varmistaa aiemmassa Orion Oyj:lle tehdyssä tutkimuksessa tehdyt havainnot sekä selvittää, mitkä tekijät vaikuttavat menetelmän soveltuvuuteen eri materiaaleille.

Työssä tutkittiin seitsemää lääketeollisuudessa käytössä olevaa geelinmuodostajaa: perunatärkkelystä, hydroksietyyliselluloosaa, hydroksipropyyliselluloosaa, kahta karbomeeriä, polyvinyylipyrrolidonia sekä polyakryyliamidia sisältävää seosta. Geelinmuodostajista ja vedestä valmistettiin näytesarjat, joiden viskositeetit mitattiin rotaatioreometrillä. Materiaaleista neljä soveltui Raman-mittauksiin valitulla mittauslaitteistolla. Raman-spektrit määritettiin hydroksipropyyliselluloosasta, karbomeereistä sekä polyvinyylipyrrolidonista. Spektrien pohjalta luotiin PLSR-mallit, joita käytettiin ennustamaan tuntemattomien näytteiden viskositeettia.

Karbomeerit soveltuivat hyvin viskositeetin mallintamiseen, ja niiden PLSR-mallit ennustivat tarkasti tuntemattomien näytteiden viskositeettia. Hydroksipropyyliselluloosan PLSR-mallin avulla ennustettujen viskositeettiarvojen vaihtelu oli suurta, eikä mallia voida pitää luotettavana. Polyvinyylipyrrolidoni puolestaan ei soveltunut PLSR-mallin luomiseen, eikä näin ollen sen viskositeettiarvoja voitu ennustaa.

Tässä tutkimuksessa varmistettiin, että Raman-spektroskopiaan ja monimuuttuja-analyysiin perustuva menetelmä soveltuu vesipohjaisten geelien viskositeetin mallinnukseen. Mallinnustulosten ja materiaalien ominaisuuksien väliltä ei kuitenkaan löydetty suoria syy–seuraussuhteita. Tärkeimmäksi tekijäksi menetelmän soveltuvuudessa eri materiaaleille osoittautuivat geelinäytteiden ulkonäkö ja konsentraatio. Jatkossa on tutkittava kattavampia näytesarjoja, joissa materiaaliominaisuuksien vaihtelu on vähäisempää. Jatkotutkimuksia on tehtävä monimutkaisemmista materiaaleista, sekä mittauslaitteiston merkityksestä viskositeetin ja Raman-spektrien määrittämisessä.

PREFACE

This thesis was done for Orion Corporation at the company's Turku plant during 2014–2015. I want to thank my supervisor Juha Jokinen and my colleague Maarit Päällysaho at Orion Corporation, without whom the whole research topic would not exist. Thank you for your efforts in providing me the opportunity to take part in this research and for the valuable advice you have given me during the whole process.

I am very grateful to my professor Helge Lemmetyinen for steering me through this thesis and for giving me more support than I could have asked for. I want to thank you for sharing a piece of the many years of experience that you have and wish you happy retirement days.

The Raman measurements were carried out at Åbo Akademi Chemistry Department in Turku, where Rose-Marie Latonen has kindly offered me her guidance in Raman spectroscopy. I am very grateful for the advice she has given me.

Taneli – thank you for your unconditional support during this time and for giving me the confidence to encounter and overcome any obstacles faced in the course of this project.

In Pori, Finland, on July 24th 2015

Saara Ostamo

TABLE OF CONTENTS

ABBREVIATIONS

CC MS	concentric cylinder measuring system
CP MS	cone-and-plate measuring system
CSR	controlled shear rate
CSS	controlled shear stress
EDA	exploratory data analysis
FT	Fourier transform
FTIR	Fourier transform infrared spectroscopy
HEC	hydroxyethylcellulose
HPC	hydroxypropylcellulose
IR	infrared
LDA	linear discriminant analysis
ME MS	Mooney/Ewart measuring system
MVA	multivariate data analysis
NIR	near infrared spectroscopy
PC	principal component
PCA	principal component analysis
PCR	principal component regression
PLS-DA	partial least squares discriminant analysis
PLSR	partial least squares regression
PP MS	parallel plate measuring system
RMSEP	root mean square error of prediction
SIMCA	soft independent modelling of class analogy
SNR	signal-to-noise ratio
SVMC	support vector machine classification
TEA	triethanolamine

α	polarizability
C_{sr}	conversion factor ($\dot{\gamma}$, n)
C_{ss}	conversion factor (τ, M)
δ_{CC}	ratio of cup and bob radii in CC MS
E	electric field
E_0	vibrational amplitude of an electromagnetic wave
E_{ph}	energy of a photon
η	shear viscosity
F	shear force
$\dot{\gamma}$	shear rate
h	Planck's constant
M	torque
n	rotational speed
ν_0	frequency of an electromagnetic wave
ν_m	vibrational frequency of a molecule
P	electric dipole moment
R_e	cup radius in CC MS
R_i	bob radius in CC MS
τ	shear stress
t	time

1. INTRODUCTION

This thesis was done for Orion Corporation at the company's Turku plant. Orion is a Finnish pharmaceutical company operating globally in developing, manufacturing, and marketing of pharmaceuticals, active pharmaceutical ingredients, and diagnostic tests [1]. The motivation for this work originates from an interest in developing a new process analytical technique for on-line quality control of gel products. A Raman spectroscopic method combined with multivariate analysis is studied for viscosity determination of aqueous gels. This is an interesting and novel research topic, on which only a few publications are found.

On-line quality control means monitoring a process in real time. In pharmaceutical industry today, many quality control procedures are executed by collecting a sample and analyzing it separately from the process. This means that any deviations in the sample quality may lead in discarding the whole batch and thus in wasting of time and money. These costs could be avoided with on-line quality control and process monitoring. [2]

Spectroscopic techniques like Fourier transform infrared (FTIR) and near-infrared (NIR) spectroscopies based on energy absorption are commonly used in quality control. They are mainly used for characterization and identification of materials, but combined with multivariate analysis methods they can also be used for quantitative analysis of chemical and physical properties, such as viscosity. FTIR provides generally more detailed information than NIR, but remote and noninvasive sampling is not possible with FTIR. With NIR, however, remote sampling and thereby on-line quality control are possible. [2]

Viscosity is an important parameter in quality control, since it provides information on product quality and consistency, end use performance, and material behavior. Viscosity measurements can also be done to assess material processability or to monitor a process during production. The conventional method for measuring viscosity is collecting a sample and measuring its flow properties with a viscometer or a rheometer. [3]

Raman spectroscopy is an interesting candidate for on-line quality control, since it combines the benefits of FTIR and NIR in addition to its unique qualities rising from the fact that Raman is a scattering technique. Raman spectroscopy has been studied in fields of process monitoring [2] and concentration assessment [4, 5]. A less investigated subject is the application of Raman spectroscopy on viscosity determination. There are studies done on the viscosity determination of aviation fuel [6], diesel [7], paint emulsions [8], and mineral oils [9, 10] with Raman spectroscopy, but no references done on

hydrogels could be found. However, a previous study done at Orion Corporation implied the possible applicability of the method on hydrogels as well [11].

The main objective of this thesis is to confirm the results of this previous study and to further investigate, whether the viscosity of different hydrogels can be modelled from Raman spectral data with multivariate methods. The second objective is to find out reasons why the method could work for some materials, but not for others. In this connection the molecular compositions and gelling mechanisms of the hydrogels are considered.

Seven viscosity increasing agents were used in preparation of the hydrogels: potato starch, hydroxylethylcellulose, hydroxypropylcellulose, two acrylic acid polymers, polyvinylpyrrolidone and a blend including polyacrylamide. A rotational rheometer was used as a conventional method to determine the reference viscosity values. A multivariate regression was used to create viscosity models from the Raman spectra. This thesis does not comprehend the construction of a robust process analytical method for final products. Only a theoretical proof for the applicability of the method is studied. In addition, instead of actual pharmaceutical products only water based hydrogels, without any additives or active ingredients are studied.

First the theoretical background of hydrogels, rheology, Raman effect, and multivariate data analysis are introduced in Section 2. Next, in Section 3, the hydrogel materials and the test methods are described in more detail. Also the execution of the analyses and the sample preparation are described in Section 3. The results and discussion are written in Section 4. Finally, Section 5 contains the conclusions and propositions for future studies.

2. THEORETICAL BACKGROUND

In this section the theoretical background of the materials and analysis methods used in this thesis are discussed. In Section 2.1 the properties of hydrogels and their pharmaceutical applications are introduced. Section 2.2 covers the principles of rheology and rheometry. Section 2.3 deals with the theory of Raman scattering and Raman spectroscopy, which is used to observe the phenomenon. Finally, Section 2.4 explains how multivariate data analysis can be utilized to find information from large and complex data sets.

2.1 Hydrogels: properties and applications

In this thesis polymer gels used in pharmaceutical applications are studied. In pharmaceutical research the term gel is often used to describe thick or non-flowing fluids in general and it does not determine the gel composition or structure [12, p. 226]. The structure may vary from thick polymer solutions to crystalline phases of a polymer or concentrated disperse systems, for example [12, p. 245]. *Hydrogel* is a common type of gel used in pharmaceuticals. Their properties, classification and applications are discussed in this section.

Hydrogels are defined as three-dimensional hydrophilic polymer networks that swell in water. Hydrogels may absorb even thousand fold their dry weight in water. Because of their high water content, hydrogels are biocompatible with proteins, living cells, and body fluids, which makes them interesting candidates for pharmaceutical applications. Hydrogels are very versatile as they can be designed to possess many different properties. [13–16]

Hydrogels cannot be unambiguously classified according to just one feature, since there are many possibilities of preparation methods and properties of hydrogels. They may be natural or synthetic in their origin, physically or chemically cross-linked, chemically stable or biodegradable, and so on. Other classification criteria include their swelling properties and porosity. In this thesis work we concentrate on finding the chemistry behind the viscosity forming properties of the gels, that is, if the gels are physical or chemical in their nature and their gelling mechanisms discussed in Section 3.1. [14, 16]

Hydrogels can be divided into chemical and physical gels. *Chemical gels* are formed by cross-linking polymer chains with covalent bonds. They are sometimes called thermoset hydrogels, because they cannot be reshaped after formation due to these covalent crosslinks. In *physical gels*, on the other hand, the crosslinks are formed by secondary forces such as hydrogen bonding, hydrophobic or ionic forces, or by entanglement of the mol-

ecules. These non-covalent junctions are reversible and as a result physical gels can be processed and they are sometimes called thermoplastic hydrogels. [14–16]

Some applications of hydrogels include contact lenses, hygiene products, tissue engineering, wound dressings, and drug delivery [15]. The latter is the main focus of this thesis and is therefore presented here in more detail. Hydrogels provide two main applications in drug delivery: controlled release and site directed drug delivery. The aim of controlled release is to maintain drug concentration in a body at an effective level for an extended period of time. This provides better therapy and reduced side effects for the patient, and increases patient's compliance and convenience as they are not bound to take the drug as often. In site directed drug release the hydrogel functions as a carrier and brings a drug to a diseased area in a body. For example, in the case of tumors or infections the drug is then able to target the diseased area directly instead of healthy organs or tissue. Site directed drug delivery systems can also be used for topical treatments. For example, certain regions in the gastrointestinal tract can be targeted through oral drug delivery, and ophthalmic drug delivery in the form of punctal plugs has been used to target the ocular surface. [13–15]

In hydrogel applications drug release may be controlled by various methods, such as diffusion, reaction, solvent, dissolution, osmosis, ion exchange, or as a response to changes in the environment. In diffusion controlled drug release the delivery device may be a reservoir or a matrix system, the both of which are described in Figure 1. In the reservoir system a drug reservoir is covered with a hydrogel membrane, through which the drug diffuses at a constant rate. In matrix systems, on the other hand, the drug is dissolved or dispersed in a three-dimensional hydrogel network and the release rate decreases with time, as the distance the drug has to travel from within the matrix increases. In solvent controlled drug release the active ingredient is incorporated in a cross-linked polymer in its glassy state. The polymer then swells in an aqueous environment, such as bio-fluids of a body, and releases the drug through diffusion. Environmentally controlled drug release can be achieved with hydrogels that are sensitive to changes in pH, temperature, light, ionic strength or the concentration of a specific molecule, for example. [13–15]

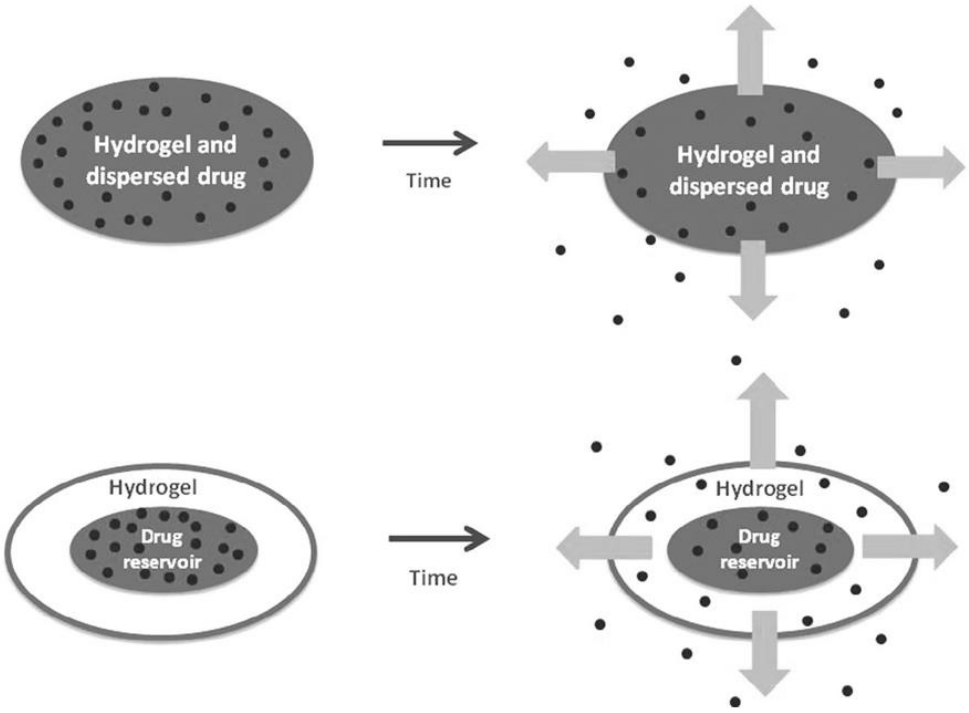

Figure 1. *Controlled drug release from a matrix system (above) and a reservoir system (below). In matrix systems the drug is dispersed in a hydrogel, from which it diffuses. In reservoir systems the drug is in a reservoir and diffuses through a hydrogel membrane. Adapted from [15].*

2.2 Rheology and flow behavior of fluids

The term *rheology* literally means "flow science". In addition to studying the flow behavior of liquids, it also investigates the deformation of solids. Rheology has its roots in physical sciences, and it was first recognized as its own branch of science in the beginning of the 20th century. All flow behavior lands in between the two extreme cases of the flow of an idealviscous liquid and the deformation of idealelastic solid. In between of these extremes are the materials that exhibit both viscous and elastic behavior, that is, they are viscoelastic. The different types of flow behavior are discussed in Sections 2.2.1–2.2.3. [17, p. 16]

Rheometry covers the methods and technology used to perform rheological measurements. Rotational and oscillatory rheometers are used to measure the flow properties of both liquids and solids. The flow properties depend on the type, degree and duration of loading as well as temperature, concentration, pH etc. Therefore measuring conditions and the measuring system have to be specified in conjunction with the results. Standardized rheometers can be used to give more comparable results. Viscous behavior is investigated by using rotational tests, whereas creep tests, relaxation tests, and oscillatory

tests are performed to study viscoelastic behavior. Section 2.2.4 deals with the rheological measurements in more detail. [17, p. 16–17]

Rheological measurements provide useful data for quality control, processability assessments, and process control, to mention a few. Often the flow behavior is easier to measure than the properties affecting it. For example, molecular weight and molecular weight distribution of polymers are difficult to measure directly, but rheological measurements can be used to help control polymer synthesis or for quality check during production. Another example is industrial construction, where viscosity plays an important role, since it affects the power needed for pumping materials and how they flow in the pipelines. In addition, rheological properties are useful in predicting the end use performance and material behavior as well as studying the effects of chemical, mechanical or thermal treatments on the material. [3]

All materials that show flow behavior, i.e. liquids and gases, are called fluids. In flowing fluids the molecules move relative to each other, which causes internal friction. The internal friction makes the fluid resist a tendency to flow to a certain extent, and this flow resistance is called viscosity. Isaac Newton postulated in 1687 that the resistance to flow of liquids is proportional to the velocity according to Newton's law,

$$\tau = \eta\dot{\gamma}, \tag{1}$$

where τ [Pa] is the shear stress, η [Pas] is the shear viscosity and $\dot{\gamma}$ [s^{-1}] is the shear rate. These are the principal rheological parameters. [17, p. 24–26]

2.2.1 Idealviscous flow behavior

The dashpot model shown in Figure 2 is used to illustrate the flow behavior of *idealviscous* fluids. When constant shear force *F* is applied on the piston, it moves continuously pressing the fluid through the gaps between the piston and the cylinder. When the load is removed, the piston remains in the reached position, i.e. the fluid remains in the deformed state. This is an irreversible process. Common idealviscous fluids are water, solvents, mineral oils, silicone oils, and blood plasma, for example. The shear viscosity of idealviscous fluids is a material constant and independent of the degree and duration of the shear load. It can be determined with flow cups, falling-ball viscometers, or capillary viscometers, for example. [17, p. 26–28]

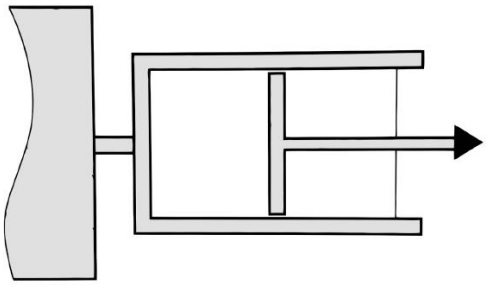

Figure 2. *The dashpot model of idealviscous fluids. [17, p. 28]*

Flow curves and viscosity curves are used for graphical presentation of measured flow behavior. The flow curve usually presents the shear stress as a function of the shear rate, while the viscosity curve presents the shear viscosity as a function of the shear rate. Viscosity curve is derived from the flow curve point by point by using Equation 1. The shear rate of idealviscous fluids is constant and thereby both flow and viscosity curves are linear. The flow and viscosity curves of idealviscous fluids are shown in Figure 3 with a solid line. [17, p. 26–28]

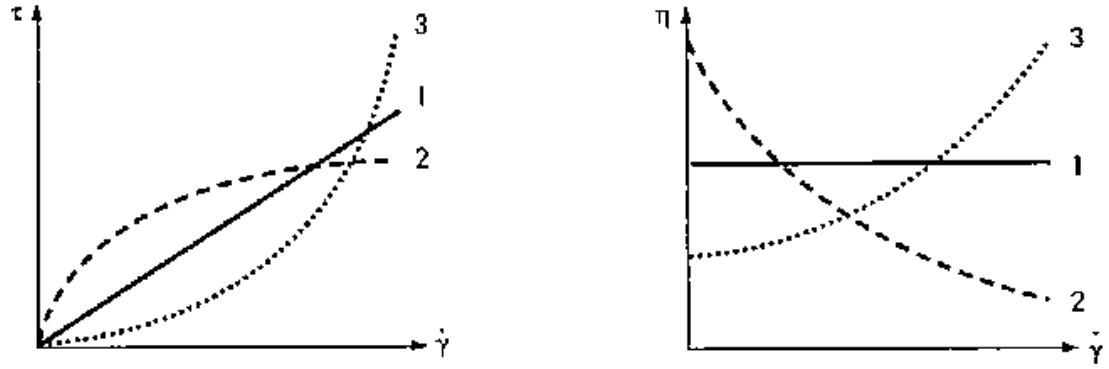

Figure 3. *The flow curves (left) and the viscosity curves (right) of idealviscous (1), shear-thinning (2), and shear-thickening (3) fluids. Adapted from [17, p. 52].*

2.2.2 Non-Newtonian flow behavior

In contrast to the idealviscous fluids, the viscosity of *non-Newtonian* fluids is affected by the shear load. If the viscosity of a fluid decreases as the shear load increases, the fluid is called *shear-thinning* or pseudoplastic. Examples of these kinds of fluids are shampoos, polymer solutions and melts, glues, and paints. On the other hand, if the viscosity increases with the shear load, the fluid is said to be *shear-thickening* or dilatant in flow behavior. Dispersions with high solids-content like ceramic suspensions or quicksand, for example, are shear-thickening fluids. Shear-thinning behavior is much more common than shear-thickening one. The representative flow curves and viscosity curves of shear-thinning and shear-thickening fluids are presented in Figure 3 with dashed and dotted lines, respectively. [17, p. 33–44]

The shear viscosity of non-Newtonian fluids is not a constant, but varies depending on the shear load. Therefore, the term apparent viscosity is used. It represents the viscosity calculated with Equation 1 at the corresponding shear rate and represents only one point of the viscosity function. For this reason the shear rate has to be informed in conjunction with the apparent viscosity values. [17, p. 34]

Some non-Newtonian fluids show a *yield point*, which means that a certain amount of force has to be applied on the material before it starts to flow. The external force F_{ext} has to be greater than the internal structural forces F_{int} of the fluid. For example dispersions and gels, like toothpaste or ketchup, show a yield point due to internal Van der Waals forces. The yield point is not a material constant, but depends on the measuring system used. [17, p. 44–45]

The reasons behind shear-thinning flow behavior depend on the type of the fluid. For polymer solutions entanglement and uncoiling under shear are proposed to explain the behavior. When at rest, the polymer macromolecules are coiled in approximately spherical form. They are entangled with themselves and with the neighboring molecules. When shear load is applied on them, the molecules start to orient in the shear direction. They uncoil and disentangle to a certain extent, which lowers their viscosity as their flow resistance becomes lower. In very low-concentrated solutions the polymers might even disentangle completely and show idealviscous behavior. Under high enough shear rates the molecules may degrade irreversibly. Also in dispersions the particles may orient in the flow direction. The interactive forces between the particles become weaker and agglomerates start to disintegrate. This again leads to lower viscosity. The structural changes in shear-thinning fluids are illustrated in Figure 4. [17, p. 35–39]

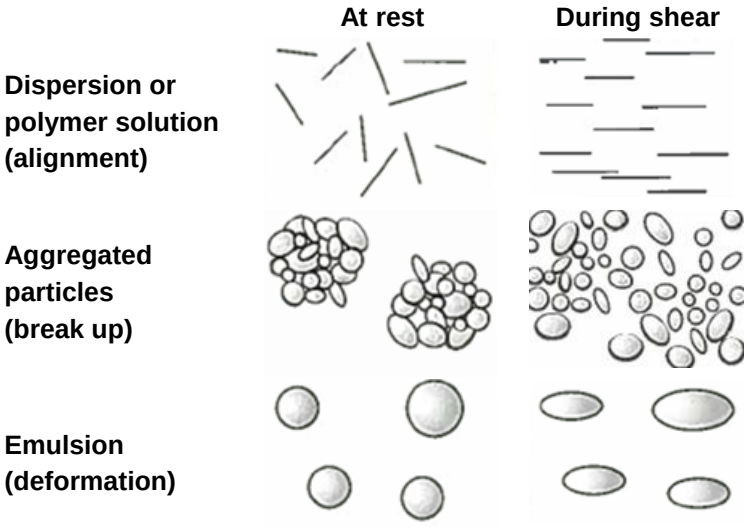

Figure 4. *Structural changes occurring in shear-thinning fluids under shear. Adapted from [17, p. 39].*

2.2.3 Time-dependent flow behavior: thixotropy and rheopexy

Almost all dispersions have *thixotropic* flow behavior. For example, when shaking a ketchup bottle, the liquid becomes thinner and flows out easier. When the shaking is stopped, the liquid starts to regain its structural strength and finally re-establishes its original consistency. In general, thixotropic fluids lose their structural strength while under shear load and regain it completely during the rest period. This is a reversible process. Many gels, paints and creams are everyday examples of thixotropic behavior as well. The term *non-thixotropic* is used to describe materials that do not recover from the shear-load-induced loss of structural strength. Non-thixotropic behavior is irreversible. The term *rheopexy*, on the other hand, describes a situation where the fluids structural strength increases under high shear. Rheopectic fluids also recover completely when left at rest, so it is a reversible process. For example, latex, casting slips, and plastisol are rheopectic fluids. [17, p. 60–61]

2.2.4 Rheometry

Rheological measurements are performed in order to investigate the flow behavior of fluids. The viscous behavior of idealviscous fluids can be determined with the viscometers mentioned in Section 2.2.1, but for non-Newtonian fluids rotational tests made with different kinds of rheometers are needed. In rotational tests either the shear rate or the shear stress is controlled. The actual raw data measured with rheometers consists of rotational speed n [min^{-1}] and torque M [Nm], from which the rheological parameters are calculated. In tests with controlled shear rate (CSR) the rotational speed of the rheometer is set and controlled, and the torque is measured as a function of it. CSR tests are used when the test sample shows no yield point. In tests with controlled shear stress (CSS), on the other hand, the torque is set and controlled and the rotational speed is recorded as a function of it. CSS tests are used when samples are showing a yield point. The measuring systems used in rotational tests are described in the following section. [17, p. 29–30]

Measuring systems

In this work, the concentric cylinder measuring system (CC MS) shown in Figure 5 is used. The CC MS consists of two concentric cylinders: the inner cylinder with radius R_i is called the bob and the outer hollow cylinder with radius R_e is called the cup. The shearing of the sample takes place in the shear gap formed between the two cylinders. In most cases the bob is the rotating part and the cup is stationary [17, p. 29]. This is called the Searle method. The Couette method, where the bob is stationary and the cup is set in motion, is more uncommon. One of the advantages of the CC MS is that it can be used for low-viscosity fluids even at high shear rates, unlike some of the other measuring systems discussed in the following. High shear rates might lead to flow instabilities,

however. The calculations involved in CC MS are described in more detail in the following subsection. [17, p. 171–172]

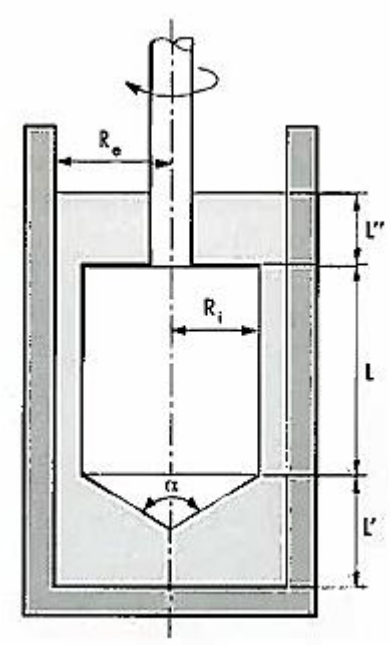

Figure 5. *Concentric cylinder measuring system. [17, p. 171]*

Another common rheometer type is the cone-and-plate measuring system (CP MS). It has a relatively flat round cone, which usually is the rotating part, located above a stationary round plate. In CP MS the shear rate is constant through the whole gap between the cone and the plate, which provides homogenous shear conditions and makes the CP MS often preferred to all other measuring systems. However, CP MS can only be used for samples with a limited maximum particle size. Therefore, CP MS cannot be used for testing gels or other samples showing three-dimensional structure. [17, p. 179–184]

In addition to these two measuring systems, there are other geometries such as parallel plate measuring system (PP MS) consisting of two even plates, and Mooney/Ewart measuring system (ME MS), which has combined cylinder and cone-and-plate geometry. The PP MS can be used for measuring dispersions with larger particle size as well as gels, for example. With rotational tests, however, the results may be inaccurate with non-Newtonian fluids, since the velocity distribution in the shear gap is not even. The ME MS is rarely used, but it can be useful when testing suspensions that are settling rapidly, for example. The purpose of having both CP and CC geometries combined is to obtain same value for shear rate in both shear gaps. [17, p. 184–190]

Calculations for CC MS

A narrow-gap CC MS is recommended, since it provides an even velocity distribution in the shear gap and thereby stable flow conditions, where the Newton's law applies. Larger shear gaps can cause turbulent flow and flow instabilities. The definitions for

narrow-gap CC MS are given by the ISO 3219 standard, which states that the ratio δ_{CC} between the radii of the cup and the bob has to be

$$\delta_{CC} = \frac{R_e}{R_i} \leq 1.0847. \quad (2)$$

In rotational tests the actual variables measured are the torque and the rotational speed as mentioned above. The corresponding shear stress and shear rate are calculated from these values using appropriate conversion factors. The shear stress is calculated from the torque by using equation

$$\tau = C_{ss} \cdot M = \frac{0.0446}{R_i^3} * M, \quad (3)$$

where C_{ss} [Pa/Nm] is the conversion factor between τ and M. The shear rate is calculated from the rotational speed according to the equation

$$\dot{\gamma} = C_{sr} \cdot n, \quad (4)$$

where C_{sr} [min/s] is the conversion factor between $\dot{\gamma}$ and n. For all ISO cylinder MS the value of C_{sr} = 1.291 min/s. The relationships between the measured and the rheological parameters are presented in Table 1. [17, p. 174–175]

Table 1. *Relationship between the raw data and the rheological parameters. Adapted from [17, p. 29].*

Raw data	Equation	Rheological parameter
Torque M	$C_{ss} \cdot M = \tau$	Shear stress τ
Rotational speed n	$C_{sr} \cdot n = \dot{\gamma}$	Shear rate $\dot{\gamma}$
	$\eta = \tau / \dot{\gamma}$	Shear viscosity η

2.3 Raman effect

Raman scattering was first observed in 1928 by C. V. Raman [18, p. 1, 19, 20]. Scattering may take place when a molecule interacts with an electromagnetic field. This interaction induces vibrational and rotational excitations, which may lead to a scattering of a photon by the molecule. [21, p. 432-434]

The classical approach to explain Raman theory involves a molecule vibrating with an electromagnetic wave. The magnitude of a time-dependent electric field E of an electromagnetic wave is given by the equation

$$E = E_0 \cos 2\pi \nu_0 t, \quad (5)$$

where E_0 is the vibrational amplitude and v_0 is the frequency of the electromagnetic wave and t indicates time. The electric field causes perturbation in the molecule as the positively charged nucleus is attracted to the negative pole and the electrons are attracted to the positive pole of the electric field. The situation is described in Figure 6 for a diatomic molecule. This charge separation induces an electric dipole moment P given by the equation

$$P = \alpha E, \tag{6}$$

where α is called polarizability and it is a proportionality constant between the dipole moment in the molecule and the magnitude of the electric field causing it [22, p. 22]. This induced dipole radiates scattered light. The primary selection rule in Raman scattering originates from the polarizability, since only vibrations that change polarizability are Raman-active. [18, p. 15–16, 20, 21, 22, p. 15–16]

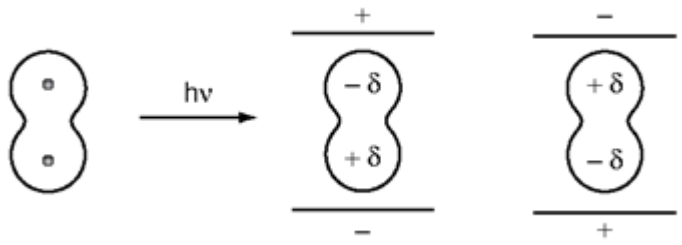

Figure 6. *Polarization of a molecule in an electric field. [22, p. 23]*

2.3.1 Rayleigh and Raman scattering

Most of the scattered light will scatter elastically, which means that they scatter at the same frequency v_0 as the incident light. This is called Rayleigh scattering and it occurs when the molecules polarizability changes with the oscillating electric field of the incident light wave. The molecule turns into a radiating dipole, as described earlier. Since the photons frequency is not affected by the scattering, the energy of the photon E_{ph} remains unchanged according to the equation

$$E_{ph} = hv, \tag{7}$$

where h is the Planck's constant. [18, p. 1–15, 20, 22, p. 15]

Raman scattering, on the other hand, is inelastic and takes place when the molecular vibrations interact with the oscillating electric field. This results in an energy difference between the incident and scattered photons corresponding to the vibrational frequency of the molecule v_m. Thus, Raman scattering has the frequencies $v_0 - v_m$ and $v_0 + v_m$, which are referred to as Stokes and anti-Stokes frequencies, respectively. [18, p. 1, 20, 21, 22, p. 15]

The spectroscopic transitions associated with different scattering processes are presented in Figure 7. In Rayleigh and Raman scattering the incident photons energy $E_{ph} = hv_0$ is chosen to be much greater than the spacing between the vibrational levels of the molecule. To visualize this, a virtual state between the ground state and the lowest excited state is introduced. The transition is depicted as an imaginary process, where the molecule absorbs a photon and transitions to a higher energy, very short-lived, virtual state and then quickly relaxes back to the ground state. [18, p. 1, 21]

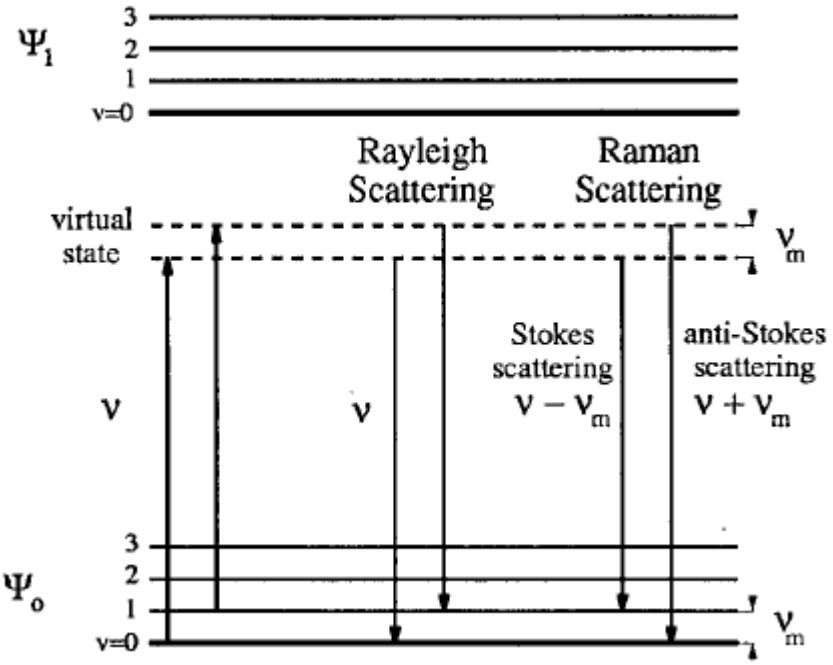

Figure 7. *Spectroscopic transitions in vibrational spectroscopy. [23, p. 36]*

In Rayleigh scattering the molecule returns to its original ground state vibrational level and scatters a photon at the same frequency as the incident light. In Stokes scattering the molecule is originally at the vibrational level $v = 0$ and transitions through the virtual state to the vibrational level $v = 1$. Scattering occurs at the frequency $v_0 - v_m$ and the molecule loses energy according to Equation 7. The anti-Stokes scattering, on the other hand, involves the small proportion of molecules, which are originally at the vibrational level $v = 1$. After scattering a photon the molecule returns to the lowest vibrational level $v = 0$ and gains energy corresponding to the scattering frequency $v_0 + v_m$. Since the population of molecules at $v = 1$ is smaller than that of $v = 0$, the anti-Stokes lines are less intense than the Stokes lines in Raman spectra. The Rayleigh peak is the most intense one and the Stokes and anti-Stokes lines are positioned symmetrically at each side of the Rayleigh peak. [18, p. 1–3, 20, 21, 22, p. 16]

Other transitions in vibrational spectroscopy are infrared (IR) absorption and fluorescence. In the IR absorption the incident photons energy matches the molecules vibra-

tional frequency and the photon is absorbed by the molecule. The molecule transitions from the lowest ground state vibrational level $v = 0$ to the vibrational level $v = 1$. Fluorescence, on the other hand, is a competitive effect of the Raman scattering. Fluorescence occurs if v_0 matches a discrete vibrational level of the excited state. The excited state molecule first decays to the lowest vibrational level of the excited state through non-radiative transitions, after which it decays back to the ground state and emits radiation, i.e. fluoresces. [22, p. 17]

2.3.2 Raman spectroscopy

Raman spectroscopy observes vibrational transitions in a molecule similarly to the IR and the near-IR (NIR) spectroscopies. The difference between these vibrational spectroscopies is that in the IR and the NIR spectroscopies the absorption of a photon is measured and in the Raman spectroscopy the scattering of a photon. There is a big difference between the probabilities of these two events, as the scattering is only 10^{-10} as likely as the corresponding mid-IR absorption. Consequently, the selection rules differ also in that a molecule is IR-active if there is a change in the dipole moment of a molecule and Raman-active if there is a change in the polarizability, as mentioned earlier. For example, totally symmetric vibrations are strong in Raman and bending vibrations are strong in IR. Similarly, vibrations of covalent bonds are often strong in Raman and vibrations of ionic bonds are stronger in IR. Although some vibrations are active in both Raman and IR, there are differences in their peak intensities. [18, p. 3–18, 22, p. 13–26, 23, p. 46]

Fourier transform (FT) IR spectroscopy is currently the most popular vibrational spectroscopy technique used. It provides high spectral resolution and the instrumentation is less expensive than that for Raman spectroscopy. However, sampling in IR spectroscopy is quite complex. For example, water and glass absorb strongly in the IR region, which restricts measurements of aqueous solutions and use of glass vials as sample holders. Sampling in IR spectroscopy is time consuming and might be destructive and it cannot be used for remote sampling. [18, p. 10, 22, p. 27]

Sampling in NIR spectroscopy, on the other hand, is easy and nondestructive. NIR is compatible with common glass and remote sampling is also possible. Water absorption is weaker than in the mid-IR region and it does not interfere with the measurements. The fundamental difference between IR and NIR is that NIR is based on overtones and combinations of the IR fundamental vibrations. This makes the NIR absorptions weaker and spectral information content poorer than in IR. [18, p. 11–12]

Raman spectroscopy is an attractive candidate for on-line process control applications, since it combines many benefits of the IR and the NIR spectroscopies. In Raman spectroscopy, fundamental vibrations are observed similarly to the IR spectroscopy and thereby high spectral information content is achieved. Raman enables easy and noninva-

sive sampling, since it is compatible with glass and water. Remote sampling is also possible. In addition, only a small sample area covering the diameter of the laser beam is needed, unlike in IR, where a lamp is used for the excitation. This has its disadvantages as well, as the laser is focused on a small area and may cause heating or photodecomposition in the sample. Other features specific to Raman spectroscopy are based on the resonance and the surface enhancements and polarization measurements. The biggest hindrance in Raman spectroscopy is the fluorescence. It is a competitive effect of scattering and even weak fluorescence may be strong enough to obscure the spectrum. [18, p. 3–12, 22, p. 26–27, 23, p. 46]

2.3.3 Instrumentation

In Raman spectroscopy the excitation source used to irradiate the sample is normally a laser operating in the UV-Vis region. A highly sensitive detector is needed to observe the scattered light, since the Raman effect is very weak. In addition to the excitation source and the detector, the instrumentation in Raman spectroscopy involves a sample holder, a sample illumination and collection system comprising of lenses and mirrors, a wavelength selector, and computer controlled processing systems. A Raman spectrum records the intensity as a function of the frequency shift between the incident light and the scattered radiation. A few factors to consider, when analyzing Raman spectra, are the signal-to-noise ratio (SNR), instrument stability and the spectral resolution, for example. [18, p. 3–73, 20, 22, p. 15–95, 23, p. 35]

The Raman instrumentation can be divided into two categories: dispersive and non-dispersive Raman spectroscopies. The instrumentation involved in these techniques is presented in Figure 8. The most common non-dispersive technique is FT-Raman spectroscopy. In dispersive Raman spectroscopy the wavelengths are scanned separately across a single detector or multiple parallel detectors. Each Raman shift is individually detected and the spectrum is formed directly by recording the number of photons hitting the detector, i.e. the intensity, as a function of the detector position. In the FT-Raman instruments, on the other hand, all the wavelengths are collected simultaneously with an interferometer and their combined signal is tracked by a single detector. The result is called an interferogram and it is demodulated by Fourier transformation to obtain the Raman spectrum. This possibility of monitoring multiple wavelengths simultaneously leads to quicker acquisition time of spectra, which is a major advantage of FT-Raman spectroscopy [18, p. 73–225, 20, 23, p. 56].

When choosing between the dispersive and the FT-Raman spectroscopies, the goal is to optimize the SNR. Often the decision is a compromise between the sensitivity and the background noise, which both affect the SNR. In general, dispersive spectrometers are usually more sensitive and have higher SNR. They use shorter laser wavelengths, which enable better sensitivity, but they are more likely to result in exciting fluorescence in the sample. FT-Raman spectrometers, on the other hand, use laser wavelengths higher than

1064 nm, which makes the measurements of fluorescing samples possible. This provides lower background noise and good frequency precision, but the SNR is lower than in the dispersive systems. A higher laser power is needed to improve the SNR, which may lead to sample heating. If fluorescence does not interfere with the measurements, the dispersive system usually provides better SNR. [18, p. 76–233, 20]

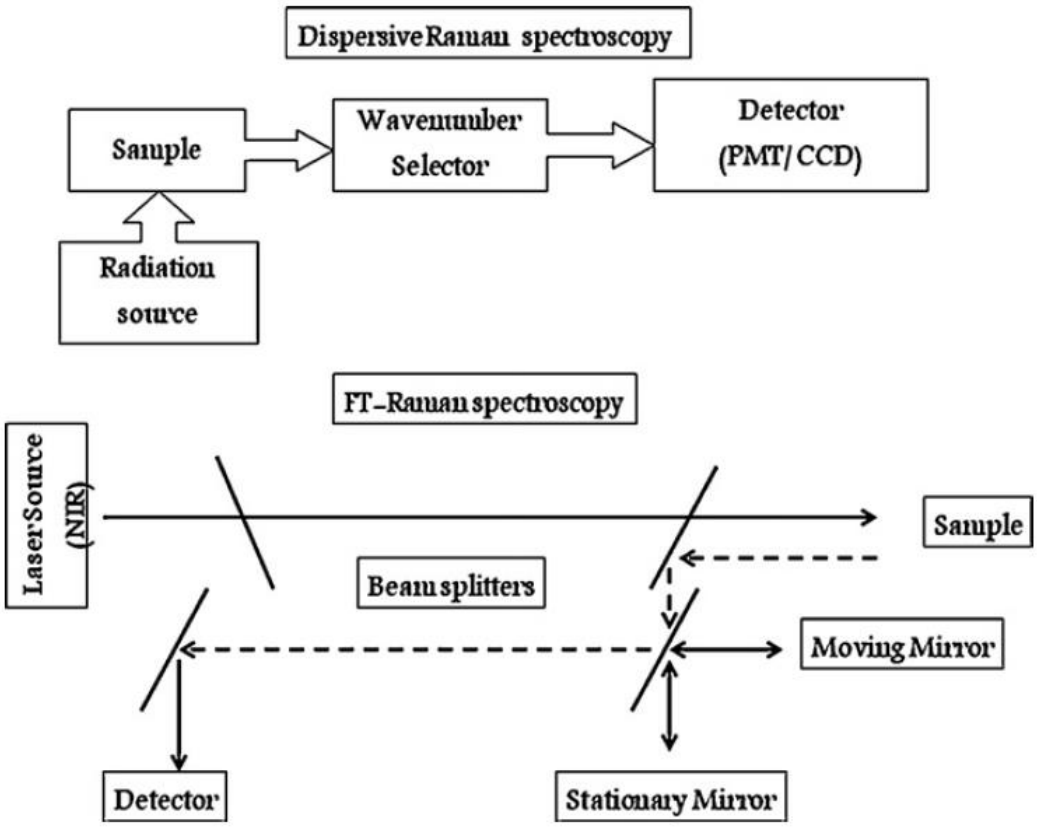

Figure 8. *Instrumentation of dispersive and non-dispersive Raman spectrometers. [20]*

2.4 Multivariate data analysis

The purpose of multivariate data analysis (MVA) is to find out what kinds of relationships, if any, exist between the multiple variables in a complex data set. The goal is to simplify the data and to find information hidden in the various correlations between the variables. In many cases univariate analysis, where the variables are assumed to be independent of each other, results in over-simplistic or over-optimistic interpretation of the data. This is because the univariate analysis cannot detect the covariance of the samples. Therefore, the study of the variability in the data and the source of it are important. In every system, there is wanted variability, i.e. controlled changes in a process that are conducted by a machine operator, for example. In addition, there is unwanted variability, the random, uncontrolled changes, to be accounted for. For analysis of both kinds of variability, multivariate models are created, which predict the future events

based on the data the model is built on. The data consists of measurements performed on samples or objects. In order to make the measurements, a set of descriptive variables is needed. [24, p. 16, 25]

The benefits of MVA lie in the identification of those variables that have the biggest influence on the variability in the data. MVA helps in isolating the variables that are related to each other and graphical presentation makes it easier to interpret the information contained in large data sets. MVA has applications in many fields of research and industry, since it is useful in the analysis of any data set comprising more than one variable. Historically it has been used in behavioral and biological sciences. Today MVA is used, for example, in marketing to study product placement, in petrochemicals to investigate gasoline blending, or in pharmaceutical development of quality by design. MVA of spectroscopic data can be used for nondestructive quality analysis of samples or raw material identification. Three different types of MVA are discussed in the following sections: exploratory data analysis, regression analysis, and classification, respectively. [24, p. 16, 25]

2.4.1 Exploratory data analysis

Exploratory data analysis (EDA) is otherwise known as data mining, since its goal is to find hidden structures in large data sets. Important patterns and groupings can be found through EDA, and it also helps in discovering if the data contain any useful information at all. In addition, EDA tries to find out the significance of different variables influencing the system. [25]

Cluster analysis aims to pattern recognition by separating the objects into clusters. The objects are clustered according to their values and the objects within one cluster are similar to each other. The clusters, on the other hand, are dissimilar and thereby differentiated from each other. On the contrary to classification, which is described in Section 2.4.3, in cluster analysis the groups and their amount are not predefined. [24, p. 451, 25]

Principal component analysis (PCA) is a data mining method, which aims in understanding relationships between samples and variables. It analyzes variability in a data set by reducing the data into *principal components* (PC). The PCs can be described as vectors defining a plane with most variability in the data space. The first PC describes the greatest source of variability, i.e. it provides the dimension along which the observations have maximal separation. The second PC is orthogonal to the first PC and describes the second greatest source of variability in the data set and so on. PCs are useful as such to find out outliers and multivariate normality, for example. The less PCs are needed to describe a data set, the better the model. In most cases, however, PCA provides the input for further analysis, such as regression analysis, which is discussed in Section 2.4.2. [24, p. 380–381, 25]

2.4.2 Regression analysis

Regression analysis aims in building a model from the measured data to predict new and future events. It requires two sets of data: independent variables and dependent variables. The independent variables are the actual measurement results and they are also called the predictors. The dependent variables, on the other hand, are the responses the model is trying to predict from the independent variables. In other words, regression analysis is the process of finding linear relationship between one or more independent variables and dependent variables. [24, p. 322, 25]

The most familiar case of regression analysis is the simple linear regression with one independent variable x and one dependent variable y. The regression surface is a straight line with the common formula $y = b_0 + b_1x$, where b_0 is a constant and b_1 is a regression coefficient or in this case, the slope. [26]

In a multiple linear regression, on the other hand, several independent variables are used to model one dependent variable. Now, a two-dimensional space is insufficient for visualization of the regression surface, although the calculations are a straightforward extension of the simple linear regression calculations. The multiple regression of i independent variables will produce an equation of the form

$$y = b_0 + b_1x_1 + b_2x_2 + \cdots + b_ix_i, \tag{8}$$

where the regression coefficients b_1–b_i describe the contributions of each independent variable to the modelled response. The actual calculations in the multiple linear regression are performed in matrix notation. [26]

Common multivariate regression methods are the partial least squares regression (PLSR) and the principal component regression (PCR). They are latent regression methods based on PCA aiming in finding hidden structure from the data set. In the latent regression methods the amount of independent variables is reduced by combining the essential effects of a group of existing variables into a new component. The main difference between PCR and PLSR is in the methods used to form the new components. PCR considers the covariance between the independent variables whereas PLSR considers the covariance between the independent and dependent variables. The most important information from data can be extracted with latent regression methods. [26]

A further extension of the multiple linear regression gives the most complex case, where in addition to having several independent variables there are also several dependent variables being modelled. This is called the multivariate multiple linear regression or the general linear model. This is beyond the scope of this thesis. For more information on the general linear model, see [24, p. 322, 26].

In order to prove that a model is suitable for its purpose, it has to be validated. The simplest and most reliable model can be found through the validation process, where the models predictive accuracy is tested. Two sample sets are needed for the testing: a calibration set and a validation set. The model is built on the samples belonging to the calibration set. The validation set is used for cross-checking whether the model performs as well in the validation set as it performs in the calibration set. [25, 26]

Common validation methods used in MVA are the test set validation and the cross-validation. If the overall sample size is large enough, the test set validation is the preferred choice. In this method a suitable portion of samples, 50–75 % for example, is separated as a calibration set and the rest is used as a validation set. The benefit of this is that the samples used in creating the model are not used in the validation. If there is an insufficient amount of samples in total to create large enough calibration and validation sets, the cross-validation method can be used. In this case all the samples are first allocated as the calibration set, from which random subsets are created. These subsets are then used as validation sets one after another until all samples have been used for both calibration and validation. [25–27]

Validation enables better interpretability of the regression analysis results and confirms that the model can be reliably used to predict future events. It also helps preventing over-fitting of the data, which means describing too much of the variation by taking non-structured variation, i.e. noise, into account. Over-fitting weakens the predictive accuracy of a model. [25–27]

2.4.3 Classification

Classification is basically separating a group of objects into one or more classes according to their characteristic features. The aim of classification in terms of MVA is to be able to identify new or existing classes from a large data set. The first step of classification is always unsupervised classification, where the objects are measured and categorized according to their similarity or dissimilarity. The next step is the supervised classification, which aims in defining rules, according which the objects are categorized. These rules are used when categorizing new objects. Classification can be used for identifying the origin of raw materials, sorting products on high-speed production lines or identifying narcotics or counterfeit products, for example. [25]

Common classification methods are the soft independent modelling of class analogy (SIMCA) and the partial least squares discriminant analysis (PLS-DA). SIMCA is based on PCA and it models the similarities of the class members. New sample is categorized into a certain class if it is similar enough to the class members, otherwise it will be discarded. PLS-DA, on the other hand, models the differences between the classes with PLS. Other classification methods are the linear discriminant analysis (LDA) and the support vector machine classification (SVMC), for example. [27]

3. MATERIALS AND METHODS

In this section, the materials and analysis methods used in this study are introduced. First, in Section 3.1 the properties of the materials used in the preparation of the hydrogel samples are described. In Section 3.2 the sample preparation is described in more detail. Sections 3.3 and 3.4 explain in how the viscosity and Raman spectroscopic measurements were carried out. Spectral processing and multivariate analysis methods are described in Section 3.5.

3.1 Materials for hydrogel preparation

Seven different materials were studied in this thesis. Short descriptions of their physical and chemical properties are provided in this section. Analytical data of the materials are presented in Table 2. The materials are listed in the table according to their trade name, and their chemical names or other synonyms are presented in the rightmost column. Their typical usage levels in solutions, solution pH, and Brookfield viscosities are also given.

In the following subsections each of the studied materials is described in more detail. Their flow properties and gel formation mechanisms are discussed. Their structural formulas and examples of their applications are also given. Any details to be taken into account with dissolution or gel preparation are also considered.

Table 2. *Analytical data of the materials. For the Brookfield viscosity and solution pH values the concentration is indicated in parenthesis.*

Trade name	Brookfield viscosity at 25 °C [mPas]	Solution pH [%]	Typical usage level [%]	Description	Synonyms / chemical name
Carbomer 980 [28]	40 000–60 000 (0.5 %)	2.5–4.0 (0.2 %)	0.5–3.0	White fluffy powder, hygroscopic, acidic	Carbopol
Carbopol 974 P [28]	29 400–39 400 (0.5 %)	2.5–4.0 (0.2 %)	0.5–3.0	White fluffy powder, hygroscopic, acidic	Carbomer
Klucel HF Pharm Hydroxypropyl-cellulose [29]	1 500–3 000 (1 %)	5.0–7.5	0–12	White to off-white powder, hygroscopic	Cellulose 2-hydroxypropyl ether
Natrosol HEC 250HR [30]	1 500–2 500 (1 %)	7	0.5–2	White to light tan powder, hygroscopic	Hydroxyethyl-cellulose / Cellulose 2-hydroxyethyl ether
Povidone K-90 [31–33]	300–700 (10 %)	4.0–7.0 (5 %)	1–20	White to creamy-white flaky powder, hygroscopic	Polyvinylpyrrolidone, 1-ethenyl-2-pyrrolidinone homopolymer
Prejel PA5 PH [31, 34]	8–10 (2 %)	4.5–7.0 (10 %)	2–12	White to off-white free flowing powder, hygroscopic	Pregelatinized starch, potato starch
Sepigel 305 [35]	1 500–4 500 (as is)	5.0–7.0 (2 %)	1–5	Translucent emulsion	Polyacrylamide / C13-14 Isoparaffin / Laureth-7

3.1.1 Carbomers: Carbopol 974P and Carbomer 980

Carbomers are high-molecular-weight acrylic acid polymers cross-linked with allyl sucrose or allyl pentaerythritol. Carbopol 974P and Carbopol 980 are highly cross-linked synthetic polymers, which makes them efficient thickeners at low concentrations. Polymerization solvent used for Carbopol 974P is ethyl acetate. Carbopol 980 is synthesized with a mixture of ethyl acetate and cyclohexane. [28, 36]

Dry carbomer molecules are tightly coiled, but they start to uncoil slightly when hydrated with water. Three-dimensionally cross-linked polymers do not dissolve in water, but

form acidic colloidal dispersions that swell and produce highly viscous microgels. Their maximum thickening ability is achieved through neutralization with a suitable base. It generates negative charges on the polymer backbone, which results in repulsion forces and uncoiling of the polymer. The most viscous gels are achieved at pH 6–11. Figure 9 demonstrates the polymer structure. [28, 31, 36]

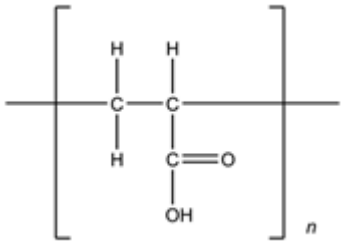

Figure 9. *Chemical structure of polyacrylic acid unit in carbomer polymers.*

Carbomer dispersions exhibit shear-thinning flow behavior, which makes them suitable excipients for many pharmaceutical and cosmetic applications. They are used as rheology modifiers and emulsifying agents in gels, creams, ointments, and lotions as well as controlled-release agents in tablet formulations. Carbomers have applications as binding agents and bioadhesives as well. [28, 31]

3.1.2 Cellulosics: Klucel HF Pharm Hydroxypropylcellulose and Natrosol 250 HR Hydroxyethylcellulose

The cellulose derivatives studied in this work are nonionic, water-soluble cellulose ethers. The cellulose molecule consists of anhydroglucose monomer units, each of which has three reactive hydroxyl groups, which can be substituted. Natrosol 250 HR Hydroxyethylcellulose (HEC) is a high-molecular-weight, high-viscosity-type cellulose ether manufactured by reacting sodium hydroxide treated cellulose with ethylene oxide to yield hydroxyethyl ether of cellulose. Klucel HF Pharm Hydroxypropylcellulose (HPC) is a high molecular weight, very low viscosity type cellulose ether. It is manufactured by reaction of alkali cellulose with propylene oxide. The structure of cellulose with its HEC and HPC derivatives are pictured in Figure 10. [29–31]

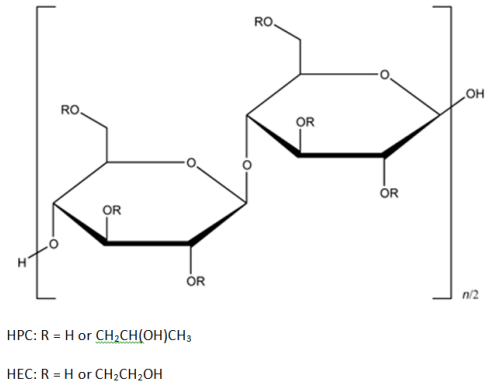

Figure 10. *Cellulose monomer unit and the substituents in HEC and HPC. Adapted from [31]*

Natrosol HEC dissolves in both hot and cold water. R-grade Natrosol HEC, however, is retarded hydration treated and therefore the dissolution time is shorter at elevated temperatures as a result of reduced hydration time. Klucel HPC on the other hand is insoluble in water above 45 °C. Solutions of the cellulose derivatives are shear-thinning with little or no thixotropy. Their viscosity increases with concentration and changes only a little at pH 2–11. [29, 30]

HEC and HPC form covalently cross-linked chemical hydrogels. They are used as thickeners and stabilizers in pharmaceutical liquids and semisolids as well as film-coating and binding agents in tablet formulations, in cosmetics creams and lotions, adhesives, and paper coatings, among others. [29–31]

3.1.3 Povidone: Kollidon K90

Povidones are synthetic polymers that consist of 1-vinyl-2-pyrrolidone monomer units presented in Figure 11. They are manufactured by free-radical polymerization of vinylpyrrolidone in water or 2-propanol. The K-values mentioned in conjunction with the names are used to describe the molecular weight of the polymer, and they are calculated from the relative viscosities of the polymers in water. The limits determined in European and US Pharmacopoeias for nominal K-values over 15 are 90–108 % of the nominal K-values. Consequently, for the nominal K-value of 90 the actual K-value can be 81.0–97.2. [33, p. 17, 26]

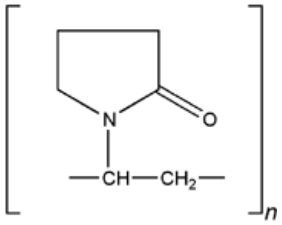

Figure 11. *The monomer unit of 1-vinyl-2-pyrrolidone. [31]*

Povidones are nonionic and water-soluble at room temperature. Kollidon K90 has high molecular weight and it forms highly viscous solutions. The viscosity is stable across wide pH range, but changes with temperature. Povidones form physical hydrogels by complex formation with water molecules. Water molecules form hydrogen-bonds with the carbonyl group of povidone [13, p. 364]. Povidones are primarily used in pharmaceuticals as binding and coating agents in tablets and capsules, but also as thickeners and stabilizers in suspensions and solutions. [31–33]

3.1.4 Starch: Prejel PA5

Prejel PA5 is a fully pregelatinised potato starch, which consists of 20–30 % amylose, the rest being amylopectin. Linear amylose and branched amylopectin pictured in Figure 12 are both polysaccharides based on α-(D)-glucose. Pregelatinised starch is obtained by mechanically or chemically breaking the starch granules. As a result of this collapse of molecular orders, irreversible changes occur, such as granular swelling, viscosity development and starch solubilization. Therefore, unlike unmodified starch, Prejel PA5 is soluble in cold water. It swells in water and forms a hydrogel through hydrogen-bonding between the amylose and amylopectin molecules. Prejel PA5 is widely used in tablet formulations, wet granulation, and as tablet and capsule binder, diluent or disintegrant. [31, 34]

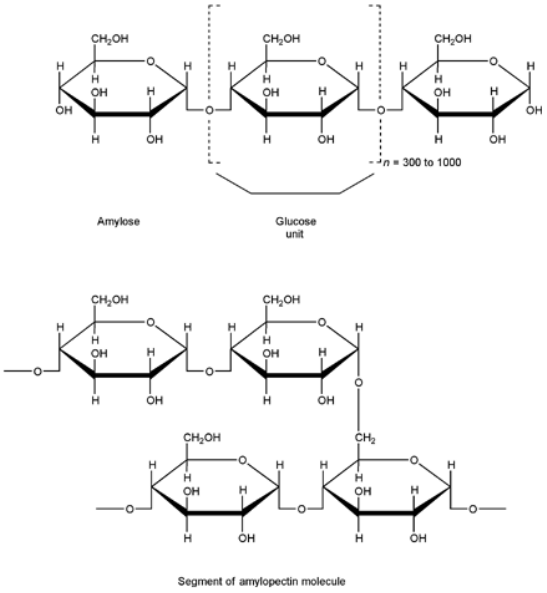

Figure 12. *Structures of amylose (above) and amylopectin (below). [31]*

3.1.5 Sepigel 305

Sepigel 305 is a blend of polyacrylamide, C13-14 isoparaffin and Laureth-7. The preneutralized polyacrylamide polymer is contained within an emulsion, where isoparaffin forms an oily phase and laureth-7 acts as a surfactant. By addition of water, the emul-

sion is inverted resulting in expanding of the polymer network and very rapid gel formation. The structure of polyacrylamide is shown in Figure 13. Sepigel 305 gels are shear thinning and non-thixotropic. They are also completely shear-resistant and their viscosity is stable over a wide pH range. Sepigel is used as an emulsifier, thickener, and stabilizer in various cosmetics applications, including gel-creams, sun products, and mascaras, for example. [35]

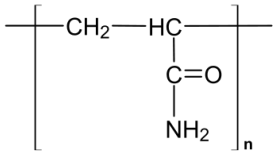

Figure 13. *Structure of polyacrylamide.*

3.2 Sample preparation

A total of 105 samples were prepared for the study. For each of the seven materials studied, three parallel sample series A, B, and C were prepared. Each series had five samples with different concentrations. All of the samples were prepared as aqueous solutions and the sample size was about 200 g. Table 3 shows the desired concentrations for each material.

Table 3. *Desired concentrations of the sample series for each material. Three parallel sample series were preapred with similar concentrations.*

	Concentration [w/v %]				
Material	**Sample 1**	**Sample 2**	**Sample 3**	**Sample 4**	**Sample 5**
Carbomer 980	0.2	0.5	1.0	1.5	2.0
Carbopol 974	0.2	0.5	1.0	1.5	2.0
HPC	1.0	5.0	10.0	12.5	15.0
HEC	0.5	1.0	1.5	2.0	2.5
Povidone	1.0	5.0	10.0	15.0	20.0
Prejel	2.0	5.0	8.0	10.0	12.0
Sepigel	0.5	1.0	1.5	2.0	3.0

The samples were prepared by first measuring 200 ml of purified water with a volumetric flask. The materials were weighed with a Mettler Toledo AT100 analytical balance. After this the water was poured from the volumetric flask into a beaker and agitated with an IKA Labortechnik RW16 Basic overhead stirrer. The weighed material was transferred gradually into the vortex created by the stirrer. Stirring time varied from 15 to 60 minutes depending on the material and the sample concentration. The time was estimated by using instructions from manufacturers and observing the sample consistency visually. The measurement record is presented in Appendix 1.

The materials were mainly added to room temperature water, except for HEC and HPC. HPC was first added to hot water (50–60 °C) to prepare a slurry, which was then cooled down to room temperature during stirring in order to dissolve the particles and form a viscous solution [29, p. 8]. Also HEC solutions were prepared in 50 °C water in order to reduce the hydratation time and thereby the total stirring time needed [30, p. 7–8]. The HEC samples were prepared by keeping the sample beaker in a 50 °C water bath during the whole stirring time.

Another exception to the basic preparation method was done with the Carbopol 974 and the Carbomer 980 samples. After dissolution of the carbomer a somewhat viscous solution was acquired. For maximum viscosity, however, the mildly acidic solution had to be neutralized. For this purpose triethanolamine (TEA) was added to the solution. The amount of TEA was measured to be approximately two times the amount of carbomer in the sample, which was the ratio recommended by the manufacturer [36]. The pH-values of Carbopol 974 and Carbomer 980 samples were measured with Mettler Toledo MP230 pH-Meter and the results were between 7 and 8. The exact values are listed in Appendix 1.

With Carbopol 974 and Carbomer 980 highly viscous solutions were achieved, which caused entrapment of air in the samples. Aeration occurred also in the Sepigel samples. The samples were kept under a vacuum for several hours. A SalvisLab Vacucenter vacuum oven was used for the purpose. The temperature was set at 25 °C and the pressure was 0–75 mbar during the deaeration.

3.3 Viscosity measurements

The viscosity measurements were performed with an Anton Paar RheolabQC rotational rheometer operating with a Searle method CC MS in Orion Corporation R&D laboratories. The cup of the measuring system CC27 was filled with the sample and the bob was immersed in it. The viscosity is highly dependent on temperature, so the system was kept at 25 °C with a temperature bath. The settling time of the system in the temperature bath was five minutes before each measurement.

RheoPlus software was used to configure the measuring profiles and to record the flow and viscosity curves of the samples. A CSR test was performed for the samples. The shear rate $\dot{\gamma}$ was controlled and the corresponding shear stress τ was recorded as a function of the shear rate. The viscosity was then calculated from these values according to Equation 1 and was also recorded as a function of the shear rate. [17, p. 29]

The general measuring profile settings used in all measurements are presented in Table 4. The measuring profiles consisted of two ramps – an increasing shear rate ramp and a decreasing one. Both ramps included 50 measuring points with 3.6 s duration. The initial and final shear rates were determined for each material separately in such a way,

that both the most concentrated and the least concentrated samples gave consistent flow and viscosity curves with the same measuring profile.

Table 4. *General measuring profile settings.*

Setting	Value
Measuring system	CC27
Number of ramps	2
Number of measuring points / ramp	50
Measuring point duration	3.6 s

First, the flow and viscosity curves of all the materials were measured with an initial shear rate of 6.5 1/s and a final shear rate of 1000 1/s. If there were inconsistencies in the end or in the beginning of the flow curve, the initial or final shear rates were increased or reduced, respectively. The shear rates used for each material are presented in Table 5.

Table 5. *Shear rates used in flow and viscosity curve measurements of each material.*

Material	Initial shear rate $\dot{\gamma}_{in}$ [1/s]	Final shear rate $\dot{\gamma}_{fin}$ [1/s]
Carbomer 980	6.5	300
Carbopol 974	6.5	300
HPC	200	1000
HEC	50	900
Povidone	100	250
Prejel	50	900
Sepigel	6.5	1000

The thicker carbomer samples were difficult to introduce evenly and without air bubbles into the measuring cylinder, which causes error in the measurements. Multiple measurements were done for some samples until consistent flow curves were obtained. This implies that the viscosity values of thicker samples are dependent on the sample handling, which was taken into account as a source of error.

3.4 Raman spectroscopic measurements

The Raman spectroscopic measurements were carried out at Åbo Akademi Chemistry Department in Turku. A Renishaw Ramascope dispersive spectrophotometer with LaserPhysics ArIon laser operating at 514 nm was used to record the Raman spectra. The laser power was set at 20 mW. A Renishaw WiRE software was used to collect the spectra. An acquisition time of 10 s and a grating of 2400 l/mm were used in the measurements of all spectra.

The gel samples were introduced in small aluminum pans covered with a microscope cover glass. A Leica DMLM microscope with an objective of focal length 15 mm was used to focus the laser on the sample. This setting provided an even gel surface leveled by the cover glass and a sufficiently air tight vessel, as the laser heated the sample and might have caused it to evaporate. The laser was focused in between the cover glass and the bottom of the aluminum vessel, as the gel itself did not give any clear focusing points. Three separate sample pans were prepared from each sample. This ensured a better coverage of the viscosity variation within one sample. Altogether 45 sample pans were thereby prepared for each material.

First, test measurements for the most concentrated samples of each material were carried out. Two laser wavelengths, 784 nm and 514 nm, were used for testing. Based on the initial test measurements, only Carbomer 980, Carbopol 974, HPC, and Povidone were decided to take under further investigation. HEC, Prejel and Sepigel did not give clear enough spectra at either laser wavelength to provide any useful information for the modelling purposes. It was decided not to measure the full spectral collection of these three materials.

For Carbomer 980 and Carbopol 974 two spectra were recorded of each sample pan resulting in a total of 90 spectra for each material. For HPC and Povidone samples three spectra were recorded of each sample pan and a total of 135 spectra were collected. The ranges of Raman shifts recorded for each material are presented in Table 6.

Table 6. *Parameters used in Raman measurements.*

Material	Raman shift [cm^{-1}]	Spectra / sample pan	Total amount of spectra
Carbomer 980	350–3500	2	90
Carbopol 974	350–3500	2	90
HPC	350–3500	3	135
Povidone	400–3500	3	135

3.5 Multivariate analysis

The multivariate analyses of the spectra were performed with the Unscrambler X software. First, spectral regions with the highest variance between the samples were identified and processed individually. The spectral regions chosen for the models are presented in Table 7. Different spectral pre-processing methods were tested, including the Savitzky-Golay smoothing, baseline offset and linear baseline correction, and area or maximum normalization. The best results for all materials were achieved by first pre-processing the spectra with the Savitzky-Golay smoothing with 0 order and 3 symmetric smoothing points and then applying the linear baseline and offset correction on them.

The PLSR was then attempted on each region separately and on combinations of multiple regions. The test set validation was used and approximately 2/3 of the spectra were used as a calibration set while the remaining 1/3 formed the validation set. The spectral data were used as predictors and the reference values of the viscosity as responses for the regression model. The reference viscosity was chosen after first forming a PLSR model with the whole viscosity curves as responses. The best modelled viscosity variable was chosen as the reference point. The shear rates corresponding to the chosen viscosity references are shown in Table 7. The number of spectra per sample and the number of spectra in calibration and validation sets used for the PLSR models of each material are also presented in Table 7.

The aim was to find the spectral regions or combinations of them, which would model the viscosity variation best in the samples and to discard the regions with high noise content. The quality of the models was evaluated based on the explained variance plots. The best models were chosen for prediction, the purpose of which is to predict viscosities of unknown samples. The same samples used in validation set were used as the unknown samples. The predicted viscosity values of the unknown samples were then compared to the actual measured viscosity values. Numbers of factors used in the prediction of each material are presented in Table 7.

Table 7. *PLSR model parameters for each material.*

	Carbomer 980	**Carbopol 974**	**HPC**	**Povidone**
Spectral ranges used in the model [cm^{-1}]	895–912 1054–1102 1150–1755 2900–2990	870–1130 1240–1730 2877–3004	827–869 1069–1169 1230–1431 1439–1482 2845–3023	724–784 821–876 921–946 1197–1512 1609–1676 2849–3030
Shear rate [1/s]	90.4	120.3	983.7	250.0
Spectra / sample	6	6	9	9
Spectra / calibration set	60	54	63	79
Spectra / validation set	30	27	36	45
Factors	3	3	3	3

4. RESULTS AND DISCUSSION

4.1 Viscosity results

The measured viscosity curves of all studied materials are presented in Appendix 2. All of the materials are shear-thinning in their flow-behavior, as their viscosity decreases as a function of the shear rate. The viscosities of HPC and Povidone decrease linearly with the increasing shear rate. The other materials lose their viscosities more rapidly as the shear stress is applied on them and their viscosities decrease close to zero as the shear rate increases.

The viscosities of the four materials, Carbomer 980, Carbopol 974, HPC, and Povidone, selected for the PLSR modelling are plotted as a function of the sample concentration in Figure 14 below. This is important to consider regarding the PLSR modelling, since it tries to make a linear fit of the variables. The viscosities of Carbomer 980 and Carbopol 974 increase linearly with the concentration. The viscosities of HPC and Povidone, on the other hand, increase in third polynomial with the increasing concentration.

The main reason for the trends in the viscosity increase is the concentration ranges used for these samples. The variation in carbomer samples is under 2 %-units, but with HPC and Povidone the variation in the concentrations are 14 and 19 %-units, respectively. The concentration ranges are chosen based on the normal usage ranges of the materials, and with carbomers high viscosity is achieved at very low concentrations.

The gelling mechanisms introduced in Section 3 cannot explain the differences between the materials in this case. Both carbomers and Povidone form physical gels, although they have different trends in the viscosity increase with the concentration. HPC on the other hand forms chemical gels through covalent bonding, but it has a similar trend in the viscosity increase with the concentration as Povidone.

In future studies the concentration range of a material should be narrowed down. In this study the sample concentration range was selected based on the manufacturer's information on possible usage levels of the material. These ranges were chosen because one aim of this study was to figure out, whether the concentration would affect the applicability of the PLSR modelling. If a commercial product's viscosity would be studied, the normal variation in products concentration would naturally narrow down the range.

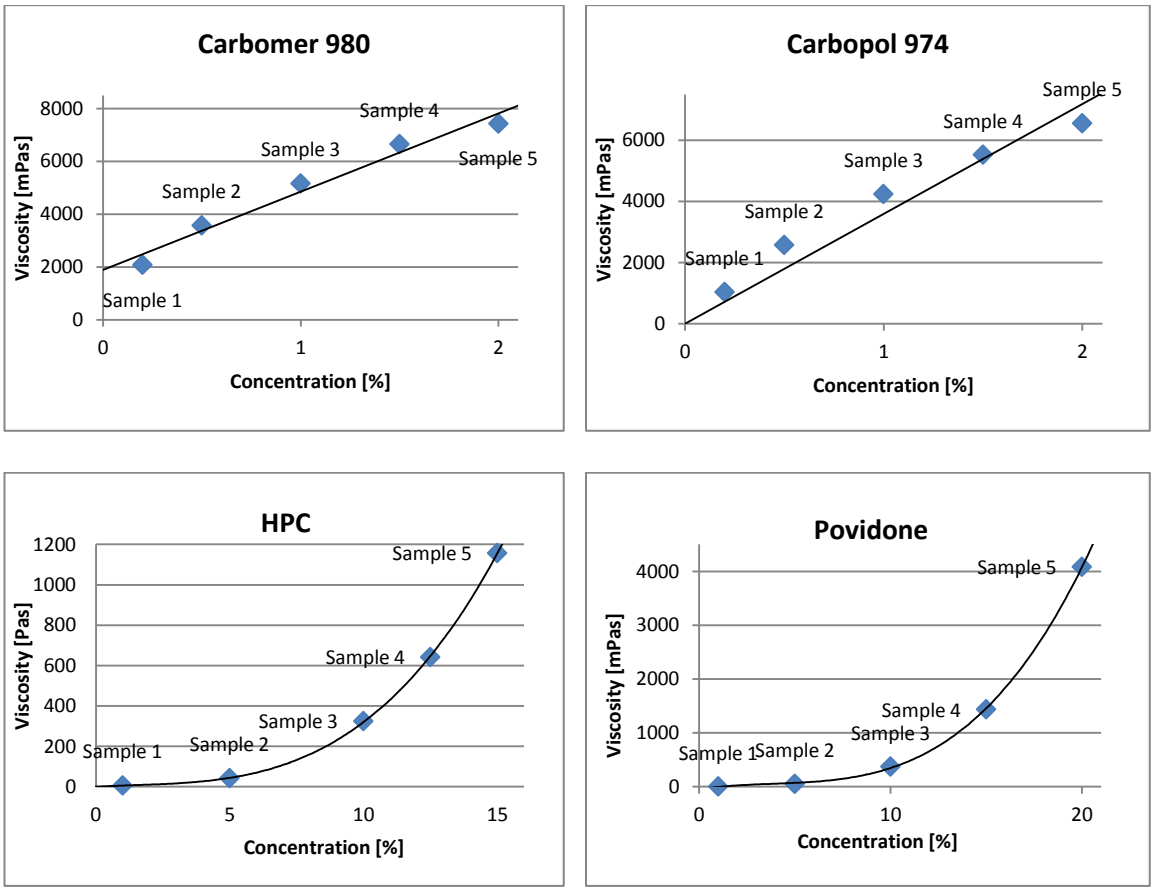

Figure 14. *The reference viscosity of Carbomer 980, Carbopol 974, HPC, and Povidone as a function of their concentration. With Carbomer 980 and Carbopol 974 the viscosity increases linearly with concentration. With HPC and Povidone the viscosity increases in third polynomial order as the concentration increases within the concentration range.*

4.2 Raman measurement results

The Raman spectra could only be measured from four materials: Carbomer 980, Carbopol 974, HPC, and Povidone. The Raman spectra of these materials are presented in Appendix 3. Prejel and Sepigel formed unclear and muddy gels. This is considered to be a hindrance in optical measurements and it prevented the collection of the Raman spectra of these materials. The fact that spectra with intensive and distinctive peaks could be measured from HPC but not from the other cellulose material, HEC, is probably caused by the different concentration ranges. The HPC sample concentration range is 1–15 %, while HEC sample concentration range is 0.5–2.5 %. Although both materials are Raman-active, the HEC samples do not include enough of the cellulose material to provide distinctive peaks in their Raman spectra. For example, the Raman spectra of 1 % HPC samples are not very distinctive, either, as can be seen in Figure 3 of Appendix 3.

The O-H stretching mode of water is clearly visible in all spectra at 3100–3650 cm^{-1}. There are also weak broad bands in all spectra around 1640 cm^{-1}, which originate from a

bending mode of the water molecule. All materials have very distinctive peaks at 2800–3000 cm^{-1} caused by the C-H stretching mode. The peaks in this range are included in the PLSR models of all materials. [37]

Other Raman shift ranges included in the PLSR models are selected from the fingerprint regions of the materials at 700–1700 cm^{-1}. All materials have CH_2 and CH_3 groups, whose symmetric and asymmetric bending modes are visible in 1400–1470 cm^{-1}. Also the C-C stretching modes are visible at 600–1300 cm^{-1}. The carbonyl stretching mode is clearly observable only in the Raman spectra of Povidone, where it overlays the H_2O bending mode. In carbomer Raman spectra the carbonyl peaks are shifted to lower frequencies and they are not as distinctive. The C-O-C symmetric stretching mode of HPC is visible at 800–970 cm^{-1} and asymmetric stretching mode at 1060–1150 cm^{-1}. [37]

4.3 Multivariate analysis results

The PLSR models were constructed with the Unscrambler X software. The interpretation of the PLSR models was based on the explained X- and Y-residuals and comparing the predicted viscosity values against the reference viscosity. Also the prediction diagnostics parameters collected in Table 8 were investigated, when choosing the best PLSR model and the number of factors used in the prediction.

Table 8. *Prediction diagnostics of the PLSR models of Carbomer 980, Carbopol 974, HPC, and Povidone.*

	Carbomer 980	Carbopol 974	HPC	Povidone
RMSEP	464.5	243.2	61.3	498.1
Bias	222.2	-17.4	2.9	-10.5
Slope	0.974	0.976	0.999	0.865
Offset	352.6	76.0	3.6	150.0
Correlation	0.978	0.992	0.989	0.947
Explained X total variance				
calibration	90.9 %	96.4 %	99.8 %	99.9 %
validation	89.7 %	96.1 %	99.7 %	99.9 %
Explained Y total variance				
calibration	96.3 %	98.6 %	97.2 %	94.0 %
validation	94.4 %	98.5 %	97.8 %	89.6 %

The slope describes the correlation between the reference and predicted viscosity values and in a good correlation it should be close to value one. The root mean square error of prediction (RMSEP) describes the expected prediction error in the same unit as the reference viscosity. The bias gives information on how the samples are located around the target line. A highly positive bias value implies a possibility of systematic error, which

predicts the values consecutively higher than the target value, and a model with a highly negative bias value predicts systematically lower values. A bias value close to zero is desired as it indicates that the samples are randomly distributed about the regression line. The offset value is the intercept of the regression curve with Y-axis, target being as close to zero as possible. The correlation is the linear correlation between the predicted and reference values, target being 1. The explained variance value tells how much of the variance is explained by a model including the corresponding the number of factors. Ideally 100 % of the variance would be explained by the model. The PLSR models and amount of factors for prediction were chosen by comparing these values and choosing the best combination of them all. [38]

In addition to the prediction diagnostics in Table 8, the interpretation of the X- and Y-variance plots of the samples was used to evaluate the fit of the model. In this study, the X-variance indicates the variance in the Raman shifts and the Y-variance describes the reference viscosity of a material. The target is to have a simple model, in which the variance is mostly described with as few factors as possible. The calibration and the validation explained variance curves should be in the best case close to each other, as this indicates a well representative model. Outliers may cause the explained validation variance to decrease with the increasing number of factors or a large gap between the validation and the calibration curves. This is not a desired effect.

Carbomer 980

The explained X- and Y-variance plots of Carbomer 980 pictured in Figure 15 indicate a well-represented model regarding both the X- and Y-variables. Most of the variance in the X-variable is described with three factors and in the Y-variable with only one factor. This is visible in the plots as a point, where a plateau is reached in the curves. Three factors are used in the prediction. The validation and calibration curves are also close to each other and no major outliers are present.

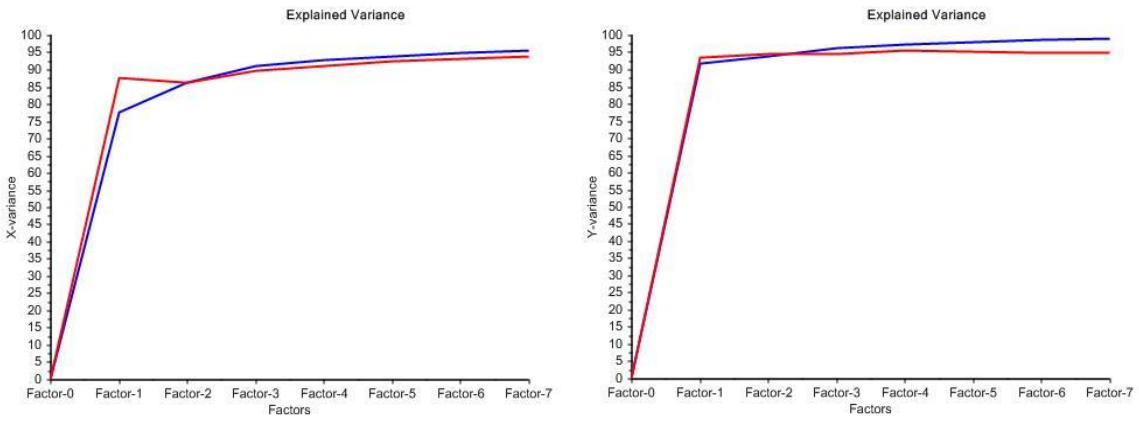

Figure 15. *Explained X-variance (left) and Y-variance (right) of the Carbomer 980 viscosity PLSR model. Explained variance of calibration is in blue and the explained variance of validation is in red.*

The prediction results of Carbomer 980 PLSR model are presented in Table 9. The deviation value states the deviation of the predicted viscosity in percentages. The prediction error is the difference of the predicted and reference viscosity values as a percentage of the reference value. The visual interpretation of the results is presented in Figure 16. Samples 2–4 have very small prediction errors and the reference viscosities are within the deviation limits of the predicted values. Sample 1 cannot be accurately predicted with this model, as the deviation is quite high as well as the prediction error. The reference value of sample 5 does not fit inside the deviation limits, but the prediction error is still considerably low. The deviation is also quite small for samples 2–5 and thereby the prediction can be considered reliable. The PLSR model works well for the Carbomer 980 samples 2–5.

Table 9. *The predicted viscosity values, the reference viscosity values, the deviation and the prediction error for Carbomer 980.*

Carbomer 980	Sample 1	Sample 2	Sample 3	Sample 4	Sample 5
Reference viscosity [mPas]	2075	3571	5159	6654	7425
Predicted viscosity [mPas]	2800 ± 481	3420 ± 396	5156 ± 399	6567 ± 447	8052 ± 537
Deviation	17 %	12 %	8 %	7 %	7 %
Prediction error	35 %	-4 %	0 %	-1 %	8 %

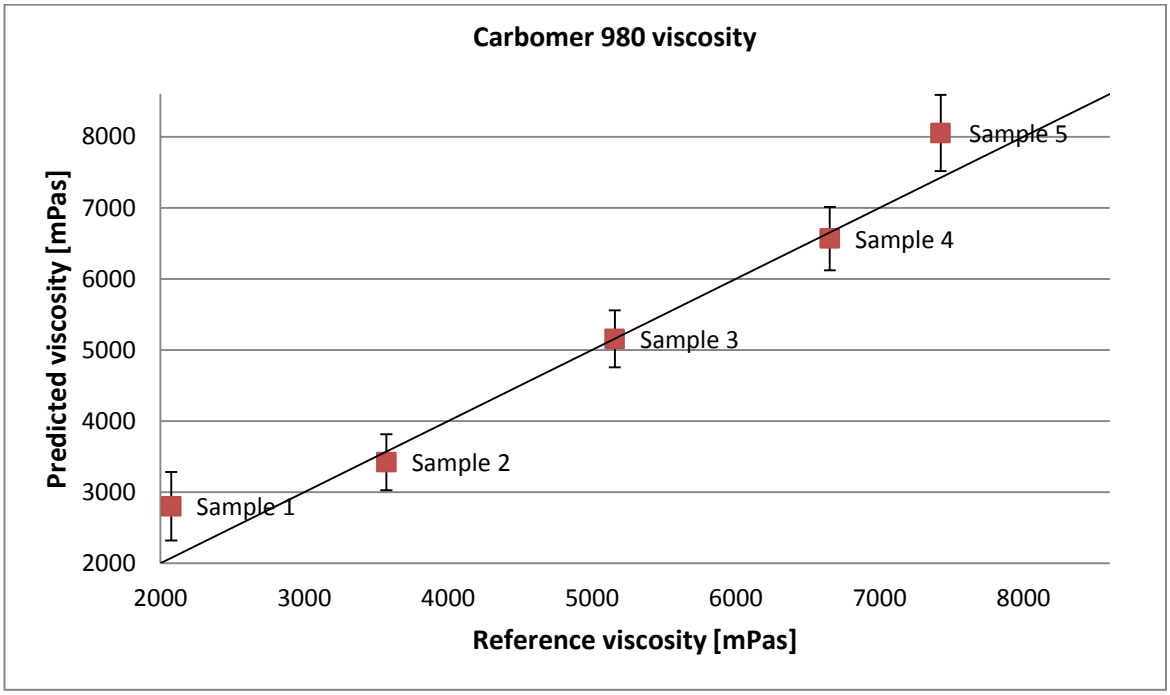

Figure 16. *The predicted viscosity of Carbomer 980 as a function of the reference viscosity. Samples 2–4 are predicted very accurately. The target line (black) does not meet the deviation limits of samples 1 and 5, but they are closely distributed about the target line.*

Carbopol 974

The explained X- and Y-variance plots of Carbopol 974 are pictured in Figure 17. Both explained X- and Y-variance plots indicate a well-represented model. Most of the variance in the X-variable is described with one factor and in the Y-variable with three factors. Three factors are used in the prediction. The validation and calibration curves are very close to each other and no major outliers are present.

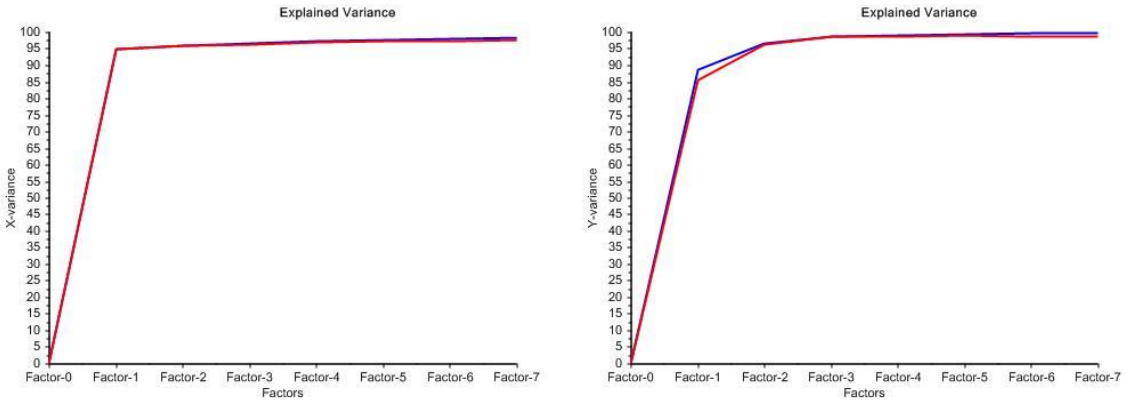

Figure 17. *The explained X-variance (left) and Y-variance (right) of the Carbopol 974 viscosity PLSR model. The explained variance of calibration is in blue and the explained variance of validation is in red.*

Table 10 presents the predicted viscosity values of Carbopol 974 with the reference values, the deviation and the prediction error for the samples. The predicted values with deviation are plotted as a function of the reference viscosity in Figure 18. All of the samples predict viscosity accurately within the deviation limits. The prediction error and deviation are small for samples 2–5 and the model predicts them very accurately. Sample 1 has a 20 % deviation, which causes the reference value to fit between deviation limits and it has quite high prediction error as well. In conclusion, the viscosity PLSR model for Carbopol 974 can accurately predict samples 2–5, but sample 1 does not fit to the model as well.

Table 10. *Predicted viscosity values with reference viscosity values, deviation and prediction error for Carbopol 974.*

Carbopol 974	Sample 1	Sample 2	Sample 3	Sample 4	Sample 5
Reference viscosity [mPas]	1031	2575	4234	5524	6544
Predicted viscosity [mPas]	1235 ± 249	2421 ± 204	4153 ± 260	5306 ± 249	6763 ± 230
Deviation	20 %	8 %	6 %	5 %	3 %
Prediction error	20 %	-6 %	-2 %	-4 %	3 %

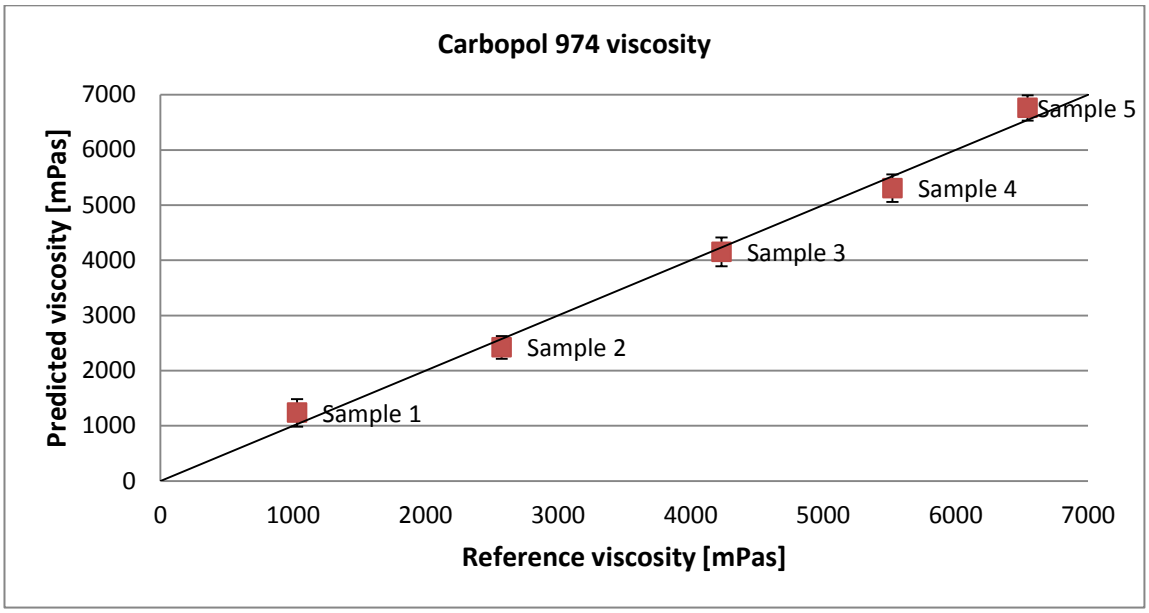

Figure 18. *The predicted viscosity of Carbopol 974 as a function of the reference viscosity. All samples are predicted very accurately.*

HPC

The explained X- and Y-variance plots of HPC are pictured in Figure 19. Both the explained X- and Y-variance plots indicate a well-represented model. Most of the variance in thr X-variable is described with one factor and in the Y-variable with three factors. Three factors are used in the prediction. The calibration and validation curves of the explained X-variance plot are almost identical and in the Y-variance plot there might be some outliers in the validation set as the explained variance decreases with the number of factors. The model can be considered representative of the samples, however.

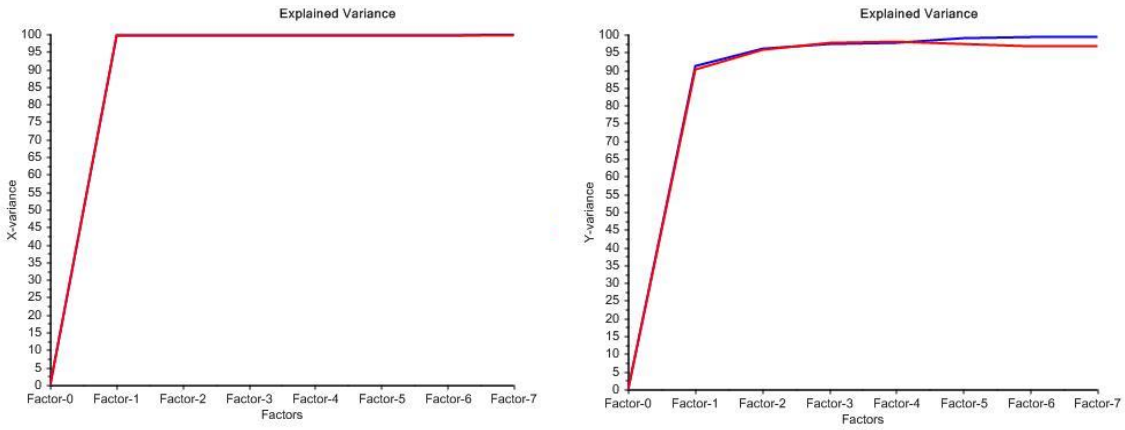

Figure 19. *The explained X-variance (left) and Y-variance (right) of the HPC viscosity PLSR model. The explained variance of calibration is in blue and the explained variance of validation is in red.*

The predicted viscosity values, the reference viscosity, the deviation and the prediction error of HPC samples are presented in Table 11. The predicted values with deviation are plotted as a function of the reference viscosity in Figure 20. Sample 1 could not be used in the PLSR model, as it could not be modelled well and it disturbed the prediction of other samples as well. The reference viscosities of samples 2, 3, and 5 fit inside the deviation limits of the predicted viscosity values. The prediction error is small for samples 3 and 5, but samples 2 and 4 have high prediction errors. The prediction is possible with the PLSR model, but it cannot be considered to be reliable. The polynomial viscosity increase with concentration causes the linear regression not to be able to fit the samples accurately.

Table 11. *The predicted viscosity values with the reference viscosity values, the deviation and the prediction error for HPC.*

HPC	Sample 1	Sample 2	Sample 3	Sample 4	Sample 5
Reference viscosity [Pas]	-	42	326	642	1157
Predicted viscosity [Pas]	-	10 ± 50	324 ± 66	741 ± 64	1102 ± 61
Deviation	-	487 %	20 %	9 %	6 %
Prediction error	-	-75 %	0 %	15 %	-5 %

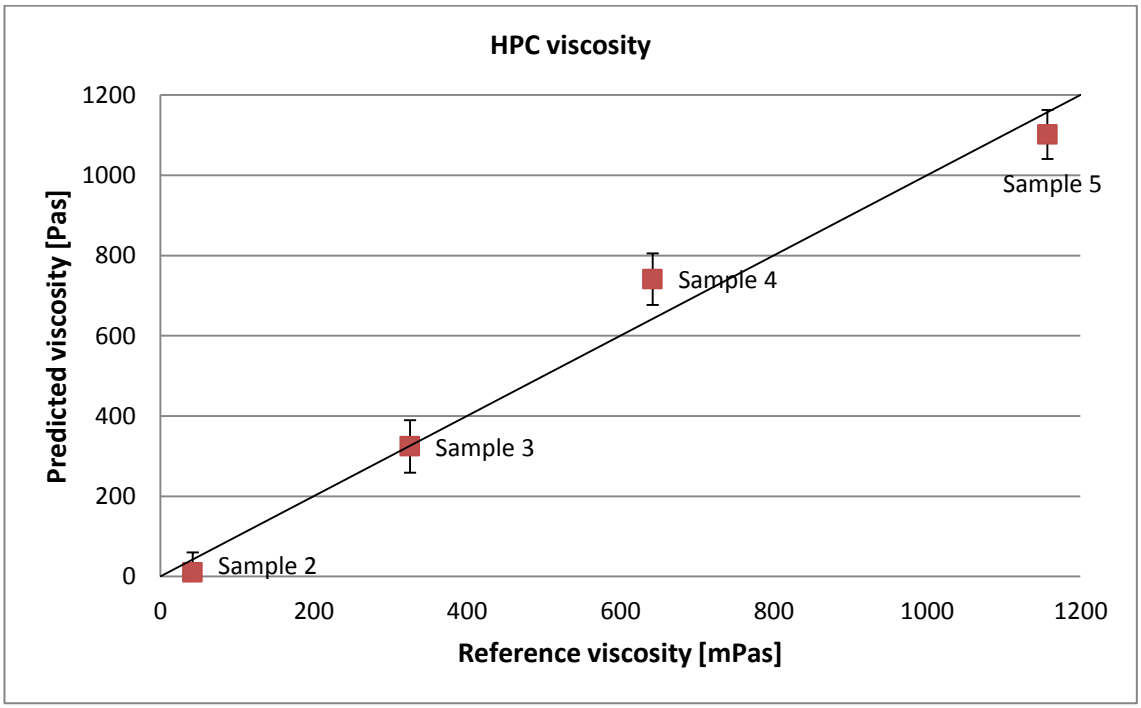

Figure 20. *The predicted viscosity of HPC as a function of the reference viscosity. The samples are evenly distributed about the target line (black), but only the reference values of samples 2, 3, and 5 are within the deviation limits.*

Povidone

The explained X- and Y-variance plots of the Povidone PLSR model are pictured in Figure 21. Most of the variance in the X-variables is explained with one factor and the calibration and validation curves are almost identical. The explained Y-variance plot on the other hand indicates that there are outliers causing the explained validation variance to decrease with increasing number of factors. Outliers causing this effect also mean that the model cannot be considered representative of the samples.

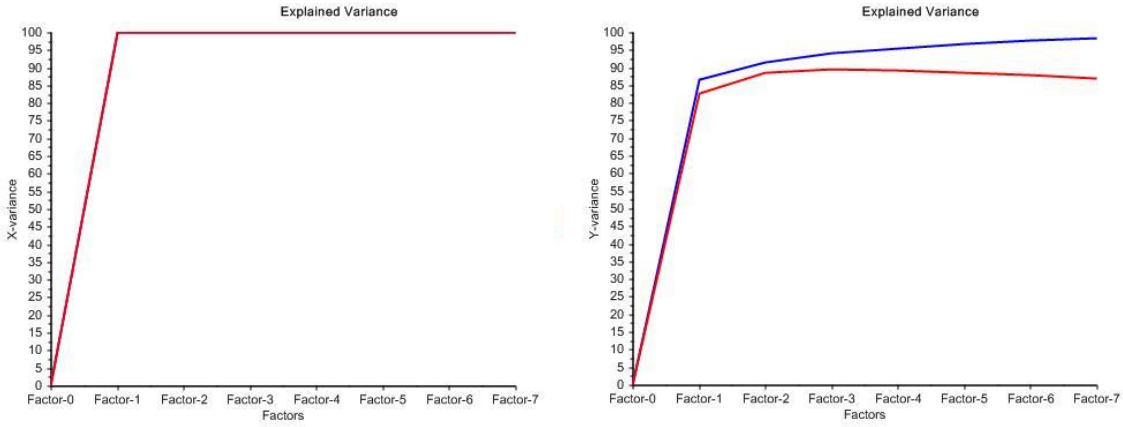

Figure 21. *The explained X-variance (left) and Y-variance (right) of the Povidone viscosity PLSR model. The explained variance of calibration is in blue and the explained variance of validation is in red.*

Prediction is attempted with three factors and the results are show in Table 12 and Figure 22. The deviations and the prediction errors of all samples are very high. The target line in Figure 22 is met by samples 1–3, but due to the large deviations this cannot be interpreted as the samples fitting the model. Povidone cannot be modelled with PLSR at this concentration range.

Table 12. *The predicted viscosity values with the reference viscosity values, the deviation and the prediction error for Povidone.*

Povidone	Sample 1	Sample 2	Sample 3	Sample 4	Sample 5
Reference viscosity [mPas]	3	51	377	1441	4082
Predicted viscosity [mPas]	-88 ± 445	-246 ± 365	776 ± 527	2019 ± 527	3440 ± 615
Deviation	-504 %	-149 %	68 %	26 %	18 %
Prediction error	-2816 %	-578 %	106 %	40 %	-16 %

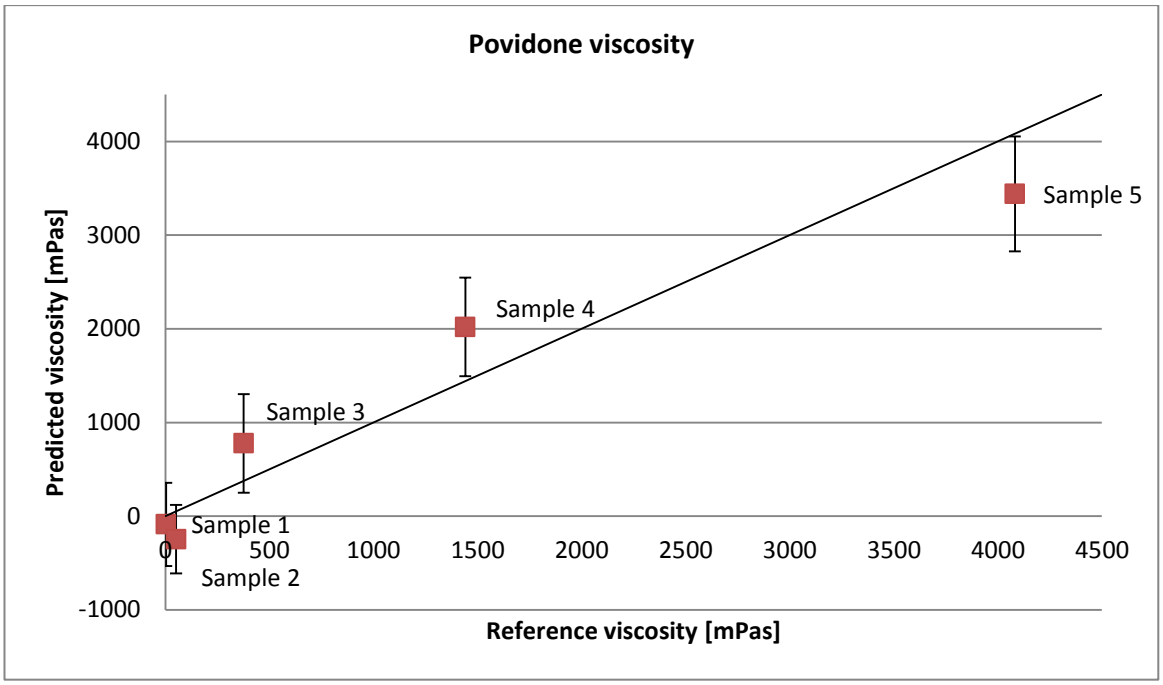

Figure 22. *The predicted viscosity of Povidone as a function of the reference viscosity. The samples are not well predicted with the model. The deviation limits are high and none of the samples fit the model well. The target line is presented with black.*

To confirm that the problems are limited only to viscosity modelling and not caused by poor spectral data, for example, a PLSR model of Povidone concentration was constructed. The explained X- and Y-variance plots of the concentration PLSR model are shown in Figure 23. Most of the variance in both X- and Y-variables is explained with one factor, and validation and calibration curves are almost identical in the explained X-variance plot as well as the explained Y-variance plot. The model is truly representative of the samples.

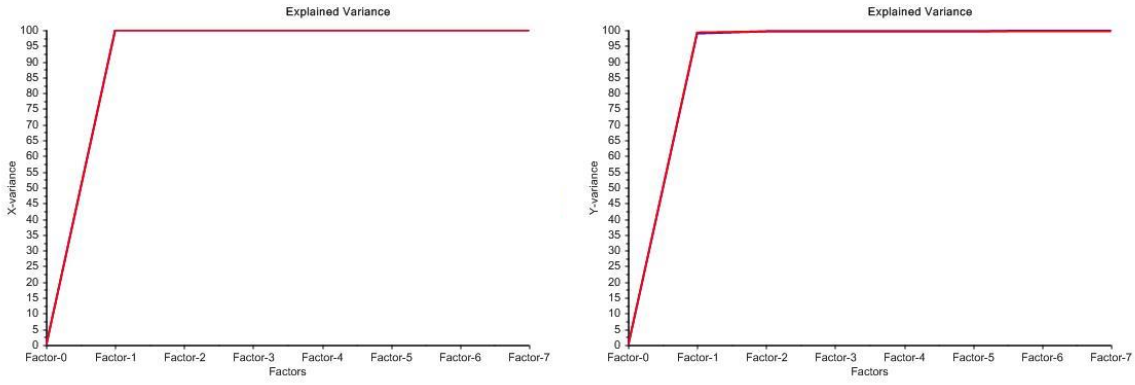

Figure 23. *The explained X-variance (left) and Y-variance (right) of the Povidone concentration PLSR model. The explained variance of calibration is in blue and the explained variance of validation is in red.*

Two factors were used in the prediction and the results are show in Table 13 and Figure 24. The model predicts very accurately all sample concentrations. The deviation in all samples is very small, although the percentage is somewhat higher in samples 1 and 2, which have the smallest concentrations. The applicability of the model on predicting concentration confirms that the Raman spectra are measured correctly and that viscosity of Povidone in the selected concentration range cannot be predicted with a PLSR model.

Table 13. *The predicted concentration values with the reference concentration values, the deviation and the prediction error for Povidone.*

Povidone	Sample 1	Sample 2	Sample 3	Sample 4	Sample 5
Reference concentration [%]	1.00	5.00	10.01	15.07	19.92
Predicted concentration [%]	1.10 ± 0.28	5.34 ± 0.23	10.05 ± 0.29	14.77 ± 0.33	19.82 ± 0.38
Deviation	10 %	7 %	0 %	-2 %	0 %
Prediction error	25 %	4 %	3 %	2 %	2 %

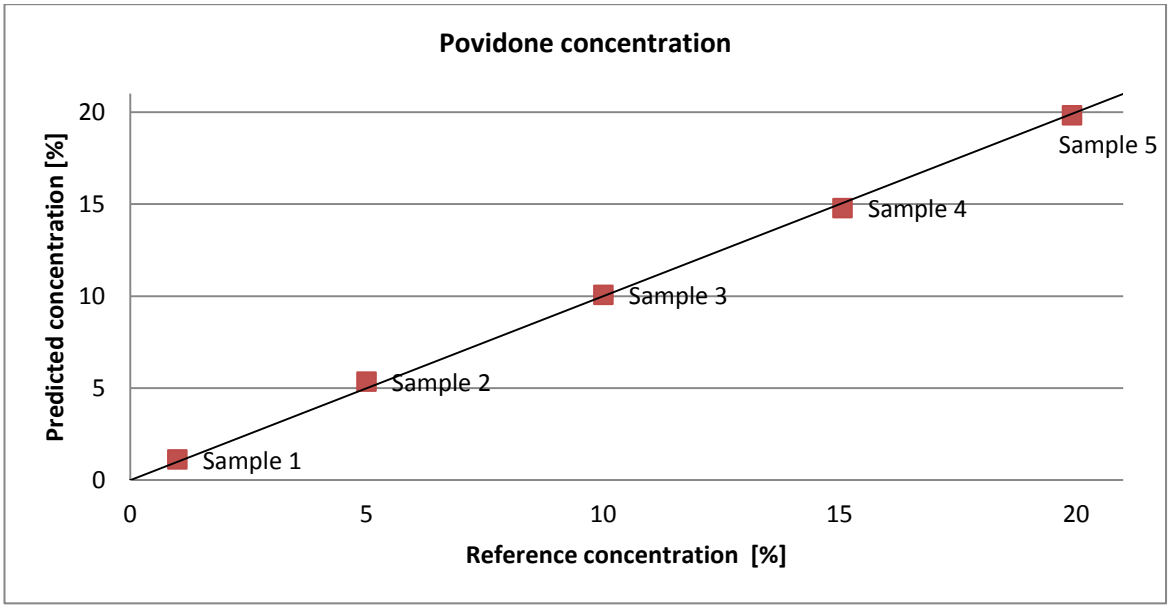

Figure 24. *The predicted concentration of Povidone as a function of the reference concentration. All samples are predicted very accurately.*

5. CONCLUSIONS

The aim of this thesis was to examine, whether it is possible to model the viscosity of aqueous gels with Raman spectroscopic methods combined with multivariate analysis. The study was conducted for the Finnish pharmaceutical company Orion Corporation, where an earlier research study had implied the applicability of the Raman spectroscopy on predicting the viscosity of hydrogels [11]. The method has been studied earlier on a few other materials, such as aviation fuel and mineral oils, but no research on modelling the viscosity of aqueous gels was found [6–10]. In this thesis, seven materials were studied to discover the factors affecting the suitability of this method for viscosity prediction.

First, the rheological properties of seven materials were measured and analyzed in order to collect reference data. However, it was possible to measure the Raman spectra of only four of the materials with the Raman spectroscopic instrumentation available. These materials, Carbomer 980, Carbopol 974, HPC and Povidone, were taken under further investigation and a PLSR model was attempted on them.

The prediction results of the PLSR models are presented below in Table 14. The accuracy of the prediction was evaluated based on the magnitude of the deviation and the prediction error values. The PLSR models of Carbomer 980 and Carbopol 974 are well representative of the samples and the models can be used for accurately predicting the viscosities of new samples. A functioning PLSR model was also achieved of HPC, but the model is not as robust or accurate in predicting the viscosities of new samples, as are the Carbomer 980 and Carbopol 974 models. In addition, the spectra of the lowest concentration samples had to be excluded from the HPC model in order to achieve more accurate prediction results. A PLSR model constructed from Povidone samples was very poor and it could not be reliably used for predicting the viscosities of new samples.

Table 14. *The prediction results of the PLSR models of Carbomer 980, Carbopol 974, HPC and Povidone. The samples range from the least concentrated one (Sample 1) to the most concentrated (Sample 5).*

	Sample 1	Sample 2	Sample 3	Sample 4	Sample 5
	Carbomer 980				
Reference viscosity [mPas]	2075	3571	5159	6654	7425
Predicted viscosity [mPas]	2800 ± 481	3420 ± 396	5156 ± 399	6567 ± 447	8052 ± 537
Prediction error [%]	35 %	-4 %	0 %	-1 %	8 %
	Carbopol 974				
Reference viscosity [mPas]	1031	2575	4234	5524	6544
Predicted viscosity [mPas]	1235 ± 249	2421 ± 204	4153 ± 260	5306 ± 249	6763 ± 230
Prediction error [%]	20 %	-6 %	-2 %	-4 %	3 %
	HPC				
Reference viscosity [Pas]	-	42	326	642	1157
Predicted viscosity [Pas]	-	10 ± 50	324 ± 66	741 ± 64	1102 ± 61
Prediction error [%]	-	-75 %	0 %	15 %	-5 %
	Povidone				
Reference viscosity [mPas]	3	51	377	1441	4082
Predicted viscosity [mPas]	-88 ± 445	-246 ± 365	776 ± 527	2019 ± 527	3440 ± 615
Prediction error [%]	-2816 %	-578 %	106 %	40 %	-16 %

The first factor affecting the applicability of the Raman spectroscopic method arose from the fact, that not all studied materials were suitable for the spectroscopic measurements. An important aspect was the appearance of the gel, as only materials forming clear gels produced distinctive Raman spectra. Thereby, the method was concluded not to be suitable for Prejel and Sepigel, which did not form clear gels. Another factor was the sample concentration, as too low proportion of the Raman-active material resulted in spectra with low-intensity peaks that could not provide any useful data for the modelling purposes.

Secondly, the concentration ranges used for the samples proved to be an important factor in constructing of the PLSR models. PLSR attempts a linear fit on the data, and therefore the viscosity and the concentration of the modelled samples should have a linear correlation. This was the case for the Carbomer 980 and Carbopol 974 samples, but not for HPC and Povidone, which had considerably wider concentration ranges. Narrowing down the concentration range would enable a linear fit between the samples. This was evident with HPC, as removing the sample with the lowest concentration enhanced the model accuracy significantly. Removing even the two lowest concentration samples from Povidone model, however, did not result in enhancement of the model accuracy. In order to emphasize the complexity of viscosity as a target property to be modelled, a PLSR model of Povidone sample concentration was constructed. The concentration model of Povidone was very accurate and had very small prediction error, as expected.

There were not enough data to make any valid conclusions on the effects of the material properties on viscosity modelling. The prediction result accuracy had no obvious correlation on the gelling mechanisms or the chemical compositions of the materials, for example. Further studies have to be carried out, where the concentration range is narrowed down to obey a linear correlation with the concentration. If a commercial product's viscosity would be studied, for example, the normal variation in products concentration would naturally narrow down the range. This kind of study could also provide a more thorough insight on how this method might be adopted in industrial processes in the future. The study should cover the effects of multiple ingredients in the gel material, effects of solvents, appearance and so on. Representative sample sets should be collected in order to have large calibration and validation sets for the model, and preferably a completely separate sample set for prediction as well. The ability to measure the reference viscosity and the Raman spectra in immediate succession would also increase the validity of the result data.

Other aspects in future studies might cover the different Raman measuring systems and the handling of gel-like samples in them, since not many references were available on the subject. Also the effect of reference the viscosity measuring system could be studied, as sample handling proved to be a possible cause of error in the rheology measurements of thicker samples. More robust results might be achieved by having a repetitive viscosity measurement method that would produce one comparable value, such as the Brookfield viscosity.

This is a novel research subject, as there were previously no other studies done on modelling viscosity of hydrogels from Raman spectral data in addition to the previous study conducted at Orion. The results achieved in this study indicate, that the viscosity of aqueous gels can be modelled from Raman spectral data with multivariate methods in suitable research conditions. It was also confirmed in this study, that the combination of Raman spectroscopy and multivariate analysis is readily suitable for concentration assessment as was already stated in [4, 5]. Various research topics should be examined before being able to apply this method in real industrial processes, but the theoretical applicability of it has been verified in this thesis. Based on the results found in this study, a novel, both cost and time saving process-analytical technique for measuring viscosity of hydrogels in real time could be developed using Raman spectroscopy accompanied by multivariate regression.

REFERENCES

[1] About Orion [WWW]. Orion Corporation. Available (accessed on 13.2.2015): http://www.orion.fi/en/Orion-group/about-orion/.

[2] Islam, M.T., Rodriguez-Hornedo, N., Ciotti, S., Ackermann, C. The potential of Raman spectroscopy as a process analytical technique during formulations of topical gels and emulsions. *Pharmaceutical research* **21** (2004) 10, pp. 1844–1851.

[3] Brookfield Engineering What Is Viscosity [WWW]. Brookfield Engineering. Available (accessed on 8.12.2014): http://www.brookfieldengineering.com/education/what-is-viscosity.asp.

[4] Tumuluri, V.S., Kemper, M. S., Lewis, I.R., Prodduturi, S., Majumdar, S., Avery, B. A., Repka, M.A. Off-line and on-line measurements of drug-loaded hot-melt extruded films using Raman spectroscopy. *International journal of pharmaceutics* **357** (2008) 1–2, pp. 77–84.

[5] Butz, J., de la Cruz, L., DiTonno, J., DeBoyace, K., Ewing, G., Donovan, B., Medendorp, J. Raman spectroscopy for the process analysis of the manufacturing of a suspension metered dose inhaler. *Journal of pharmaceutical and biomedical analysis* **54** (2011) 5, pp. 1013–1019.

[6] Andrade, J.M., Garrigues, S., de la Guardia, M., Gómez-Carracedo, M., Prada, D. Non-destructive and clean prediction of aviation fuel characteristics through Fourier transform-Raman spectroscopy and multivariate calibration. *Analytica Chimica Acta* **482** (2003) 1, pp. 115–128.

[7] Santos Jr., V.O., Oliveira, F. C.C., Lima, D.G., Petry, A.C., Garcia, E., Suarez, P.A.Z., Rubim, J.C. A comparative study of diesel analysis by FTIR, FTNIR and FT-Raman spectroscopy using PLS and artificial neural network analysis. *Analytica Chimica Acta* **547** (2005) 2, pp. 188–196.

[8] Ito, K., Kato, T., Ona, T. Rapid viscosity determination of waterborne automotive paint emulsion system by FT-Raman spectroscopy. *Vibrational Spectroscopy* **35** (2004) 1–2, pp. 159–163.

[9] Mooeung, K., Hoeil, C. Enhancement of the spectral selectivity of complex samples by measuring them in a frozen state at low temperatures in order to improve accuracy for quantitative analysis. Part II. Determination of viscosity for lube base oils using Raman spectroscopy. *Analyst* **138** (2013) 5, pp. 1515–1522.

[10] Mooeung, K., Sanguk, L., Kyeol, C.H., C., Young, M.J. Use of temperature dependent Raman spectra to improve accuracy for analysis of complex oil-based samples: Lube base oils and adulterated olive oils. *Analytica Chimica Acta* **748** (2012), pp. 58–66.

[11] Päällysaho, M. Process Analytical Techniques (PAT) for Manufacturing and Packaging Pharmaceutical Semisolids. Master's thesis. Turku 2013, Lappeenranta University of Technology. 101 p.

[12] Malmsten, M. Surfactants and Polymers in Drug Delivery. New York, USA 2002, Marcel Dekker. 348 p.

[13] Fried, J.R. Polymer Science and Technology. 2nd ed. NJ, US 2003, Pearson Education, Inc. 582 p.

[14] Uchegbu, I.F., Schätzlein, A.G. (ed.). Polymers in Drug Delivery. Boca Raton, FL, USA 2006, CRC Press, Taylor & Francis Group. 259 p.

[15] Caló, E.,Khutoryanskiy, V.V. Biomedical applications of hydrogels: A review of patents and commercial products. *European Polymer Journal* **65** (2015), pp. 252-267.

[16] Hoffman, A.S. Hydrogels for biomedical applications. *Advanced Drug Delivery Reviews* **54** (2002) 1, pp. 3–12.

[17] Mezger, T.G. The Rheology Handbook: For users of rotational and oscillatory rheometers. 2nd ed. Hannover, Germany 2006, Vincentz Network. 299 p.

[18] McCreery, R.L. Raman Spectroscopy for Chemical Analysis. Hoboken, NJ, USA 2000, John Wiley & Sons, Inc. 420 p.

[19] G.F.S. A new radiation. *Journal of the Franklin Institute* **206** (1928) 2, pp. 276–277.

[20] Das, R.S., Agrawal, Y.K. Raman spectroscopy: Recent advancements, techniques and applications. *Vibrational Spectroscopy* **57** (2011) 2, pp. 163–176.

[21] Engel, T., Reid, P. Physical Chemistry. 2nd ed. NJ, US 2010, Pearson Education, Inc. 1067 p.

[22] Ferraro, J.R., Nakamoto, K., Brown, C. Introductory Raman Spectroscopy. 2nd ed. Burlington, USA 2003, Elsevier Science. 434 p.

[23] Jirasek, A. Fourier Transform Raman Spectroscopy of Polyacrylamide Gels for Use in Radiation Dosimetry. Vancouver, Canada 2002, The University of British Columbia. 180 p.

[24] Rencher, A.C. Methods of Multivariate Analysis. 2nd ed. NY, US 2002, John Wiley & Sons, Inc. 708 p.

[25] Swarbrick, B. Multivariate Data Analysis for Dummies, CAMO Software Special Edition. Chichester, West Sussex 2012, John Wiley & Sons, Ltd. 31 p.

[26] StatSoft, I. Electronic Statistics Textbook [WWW]. Tulsa, OK 2013, StatSoft. Available (accessed on 7.1.2015): http://www.statsoft.com/textbook/.

[27] Glossary of Multivariate Statistical Methods [WWW]. CAMO Software AS. Available (accessed on 9.1.2015): www.camo.com/downloads/Glossary_of_terms.pdf.

[28] Pharmaceutical Polymers for Liquid and Semisolid Dosage Forms. 2011, Lubrizol Advanced Materials, Inc. 11 p.

[29] Klucel™ Hydroxypropylcellulose Physical and Chemical Properties. 2012, Ashland Specialty Ingredients. 23 p.

[30] Natrosol® Hydroxyethylcellulose Physical and Chemical Properties. 1999, Hercules Inc. 20 p.

[31] Sheskey, P.J., Cook, W.G., Cable, C.G. Handbook of Pharmaceutical Excipients [WWW]. Pharmaceutical Press and American Pharmacists Association 2014. Available (accessed on 27.11.2014): https://www.medicinescomplete.com/mc/excipients/current/.

[32] Plasdone Povidones Product Overview. 2009–2013, Ashland Inc. 4 p.

[33] Bühler, V. Kollidon - Polyvinylpyrrolidone Excipients for the Pharmaceutical Industry. 9th ed. Ludwigshafen, Germany 2008, BASF. 328 p.

[34] The Binding Performance of DFE Pharma Starch. 2013, DFE Pharma. 7 p.

[35] Sepigel 305 Emulsifying-Thickening Polymer. 2007, SEPPIC. 38 p.

[36] The Proven Polymers in Pharmaceuticals. 1994, BFGoodrich.

[37] Raman Spectroscopy for Analysis and Monitoring [WWW]. HORIBA Jobin Yvon Inc. Edison. Available (accessed on 28.6.2015): http://www.horiba.com/fileadmin/uploads/Scientific/Documents/Raman/bands.pdf.

[38] The Unscrambler X Help. Oslo 2013, CAMO Software.

[39] Shiley, D. Quantitative Prediction of Material Properties Using Reflectance Spectroscopy: A Multivariate Chemometrics-based Approach. Proceedings of ASD and IEEE GRS; Art, Science and Applications of Reflectance Spectroscopy Symposium, Vol. II, Boulder, CO, USA, February 23–25, 2010. Boulder, CO 2010. 10 p.

APPENDIX 1: SAMPLE PREPARATION

The measurement record of sample preparation is presented here. The weighed amount of the viscosity increasing agent and the actual concentration of the samples are presented in the following Tables 1–7 for each material. In addition, the stirring times for each material and the pH of the Carbomer 980 and Carbopol 974 samples are also presented in below.

Table 1. *Preparation of Carbomer 980 samples. Stirring time indicates first the dispersion time of the carbomer and then the stirring time after the addition of TEA.*

Carbomer 980	**m [g]**	**c [w/v %]**	**pH**
A1	0.40	0.20	7.96
B1	0.40	0.20	7.94
C1	0.40	0.20	7.90
A2	1.00	0.50	7.78
B2	1.01	0.50	7.78
C2	1.01	0.50	7.63
A3	2.02	1.00	7.61
B3	2.03	1.00	7.46
C3	2.02	1.00	7.45
A4	3.06	1.51	7.43
B4	3.04	1.50	7.46
C4	3.04	1.50	7.33
A5	4.10	2.01	7.53
B5	4.08	2.00	7.43
C5	4.09	2.00	7.48
Stirring time	20 + 5	min	

Table 2. *Preparation of Carbopol 974 samples. Stirring time indicates first the dispersion time of the carbomer and then the stirring time after the addition of TEA.*

Carbopol 974	m [g]	c [w/v %]	pH
A1	0.40	0.20	7.97
B1	0.40	0.20	7.93
C1	0.41	0.20	8.01
A2	1.00	0.50	7.89
B2	1.01	0.50	7.91
C2	1.01	0.50	7.79
A3	2.07	1.02	7.73
B3	2.03	1.00	7.68
C3	2.02	1.00	7.63
A4	3.05	1.50	7.69
B4	3.06	1.51	7.61
C4	3.05	1.50	7.71
A5	4.07	1.99	7.66
B5	4.08	2.00	7.51
C5	4.08	2.00	7.46
Stirring time	20 + 5 min		

Table 3. *Preparation of HEC samples.*

HEC	m [g]	c [w/v %]
A1	1.02	0.51
B1	0.99	0.49
C1	1.00	0.50
A2	2.03	1.01
B2	2.02	1.00
C2	2.03	1.01
A3	3.07	1.51
B3	3.03	1.49
C3	3.05	1.50
A4	4.08	2.00
B4	4.08	2.00
C4	4.09	2.00
A5	5.13	2.50
B5	5.13	2.50
C5	5.13	2.50
Stirring time	30 min	

Table 4. *Preparation of HPC samples.*

HPC	m [g]	c [w/v %]
A1	2.07	1.02
B1	2.07	1.02
C1	2.06	1.02
A2	10.60	5.03
B2	10.55	5.01
C2	10.48	4.98
A3	22.25	10.01
B3	22.11	9.96
C3	22.11	9.96
A4	28.49	12.47
B4	28.56	12.49
C4	28.50	12.47
A5	35.48	15.07
B5	35.25	14.98
C5	35.20	14.96
Stirring time	15 min	

Table 5. *Preparation of Povidone samples.*

Povidone	m [g]	c [w/v %]
A1*	2.03	1.01
B1*	2.00	1.00
C1*	1.99	1.00
A2**	10.00	5.00
B2**	10.00	5.00
C2**	9.99	4.99
A3	22.24	10.01
B3	22.29	10.03
C3	22.26	10.01
A4	35.50	15.07
B4	35.29	15.00
C4	35.93	15.23
A5	49.75	19.92
B5	49.98	19.99
C5	49.98	19.99
Stirring time	30 min	

*V(H2O)=198 ml

**V(H2O)=190 ml

Table 6. *Preparation of Prejel samples*

Prejel	m [g]	c [w/v %]
A1	4.09	2.00
B1	4.10	2.01
C1	4.07	2.00
A2	10.57	5.02
B2	10.51	4.99
C2	10.54	5.01
A3	17.41	8.01
B3	17.39	8.00
C3	17.37	7.99
A4	22.20	9.99
B4	22.25	10.01
C4	22.22	10.00
A5	27.24	11.99
B5	27.27	12.00
C5	27.29	12.01
Stirring time	60	min

Table 7. *Preparation of Sepigel samples.*

Sepigel	m [g]	c [w/v %]
A1	1.09	0.54
B1	1.06	0.53
C1	1.02	0.51
A2	2.06	1.02
B2	2.09	1.03
C2	2.04	1.01
A3	3.06	1.51
B3	3.08	1.52
C3	3.10	1.53
A4	4.08	2.00
B4	4.08	2.00
C4	4.07	2.00
A5	6.14	2.98
B5	6.18	3.00
C5	6.20	3.01
Stirring time	15	min

APPENDIX 2: VISCOSITY RESULTS

The viscosity curves of the studied materials are presented below in Figures 1–7. All of the materials are shear-thinning in their flow-behavior, as their viscosity decreases as a function of the shear rate. The viscosities of Povidone and HPC decrease linearly with increasing shear rate. The other materials lose their viscosities quickly after shear stress is applied on them and their viscosities decrease close to zero as the shear rate increases.

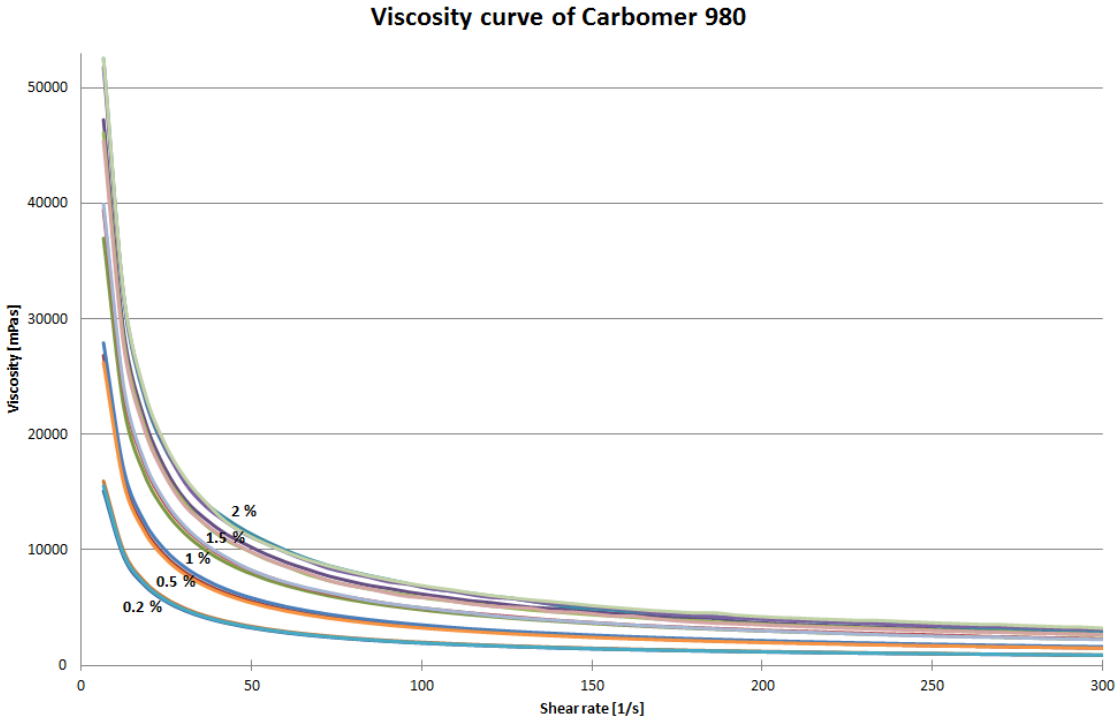

Figure 1. *Viscosity of Carbomer 980 as a function of shear rate. Viscosity decreases close to zero as the shear rate increases to its maximum.*

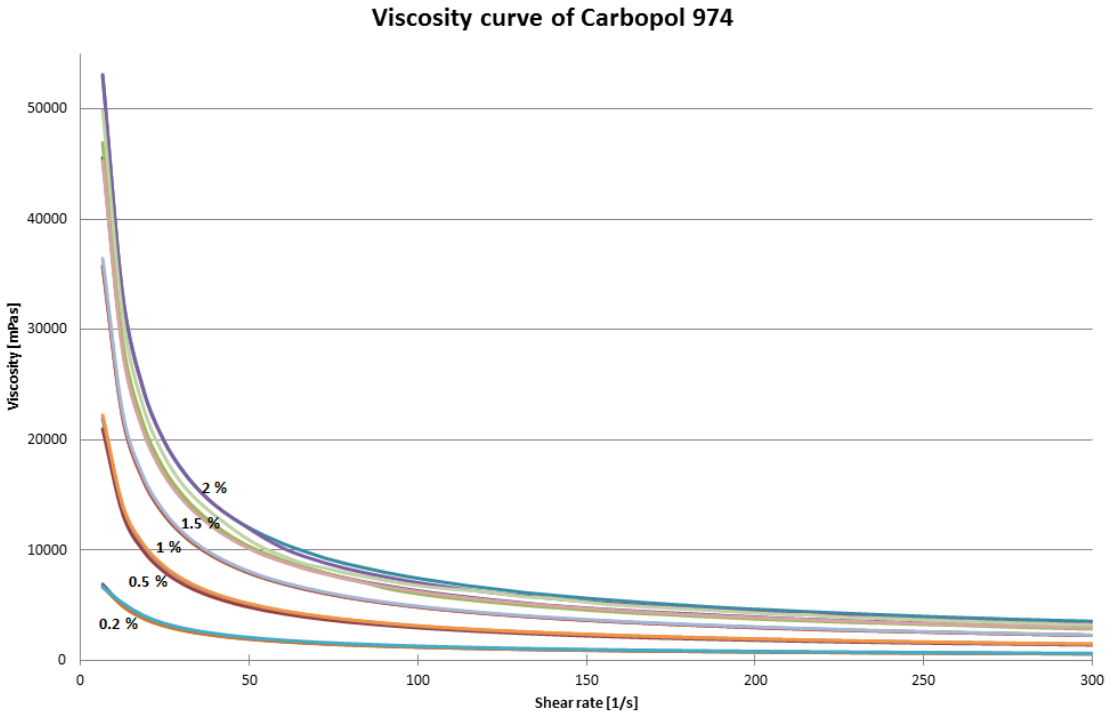

Figure 2. *Viscosity of Carbopol 974 as a function of shear rate. Viscosity decreases close to zero as the shear rate increases to its maximum.*

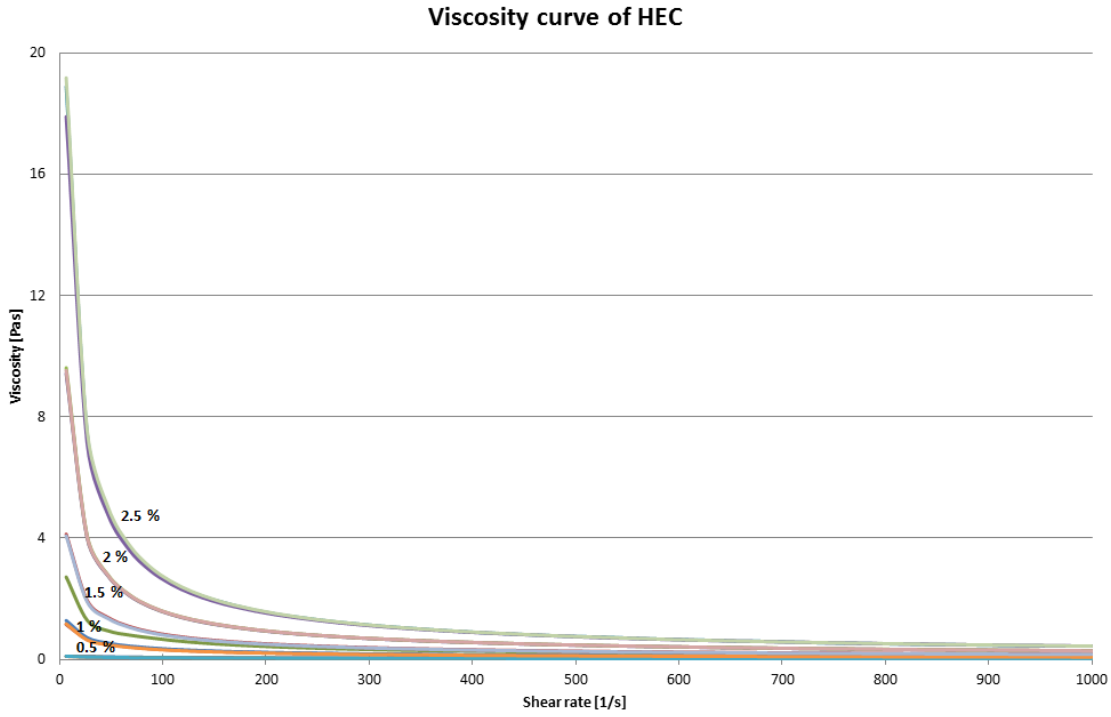

Figure 3. *Viscosity of HEC as a function of shear rate. Viscosity decreases close to zero as the shear rate increases to its maximum.*

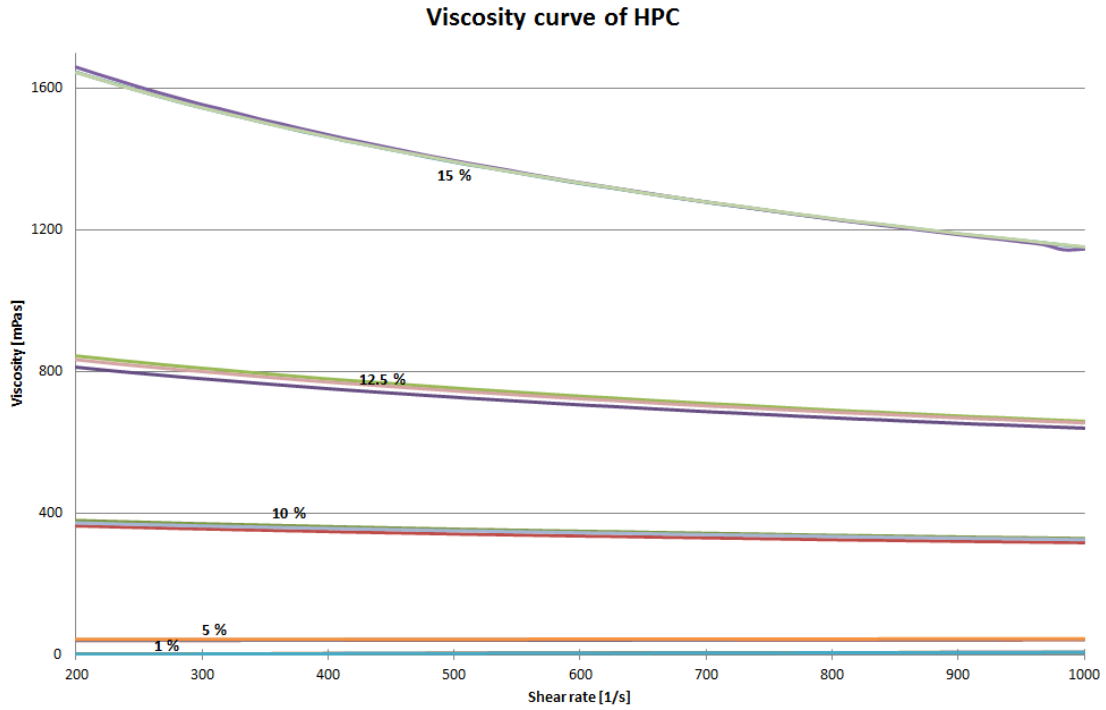

Figure 4. *Viscosity of HPC as a function of shear rate. Viscosity decreases linearly as the shear rate increases.*

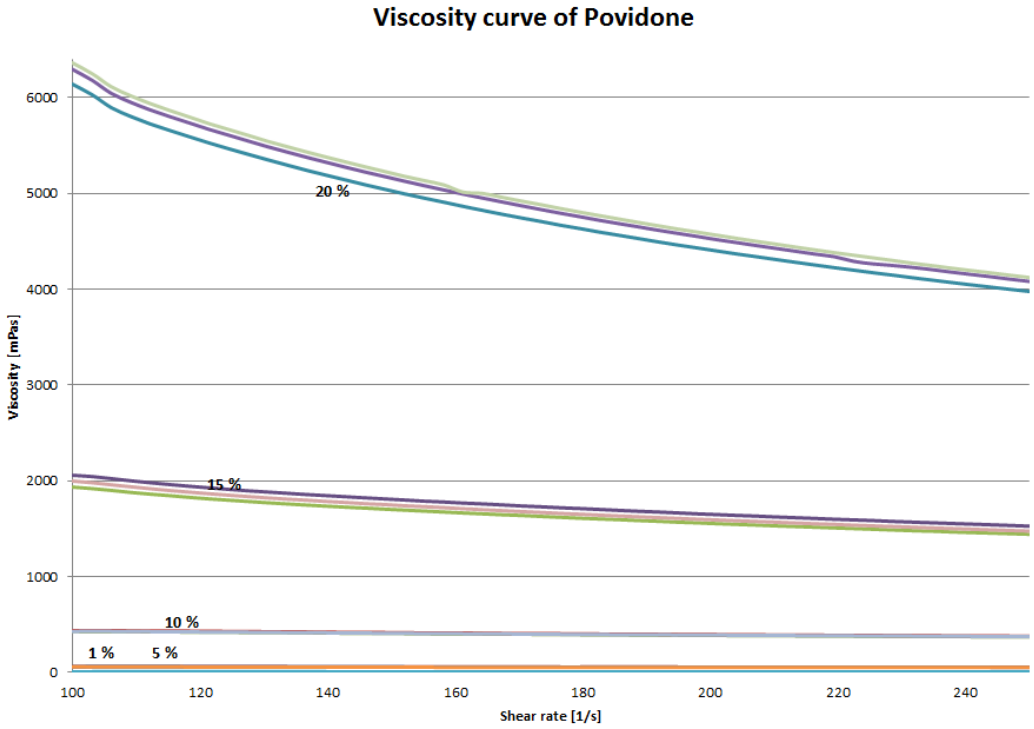

Figure 5. *Viscosity of Povidone as a function of shear rate. Viscosity decreases linearly as the shear rate increases.*

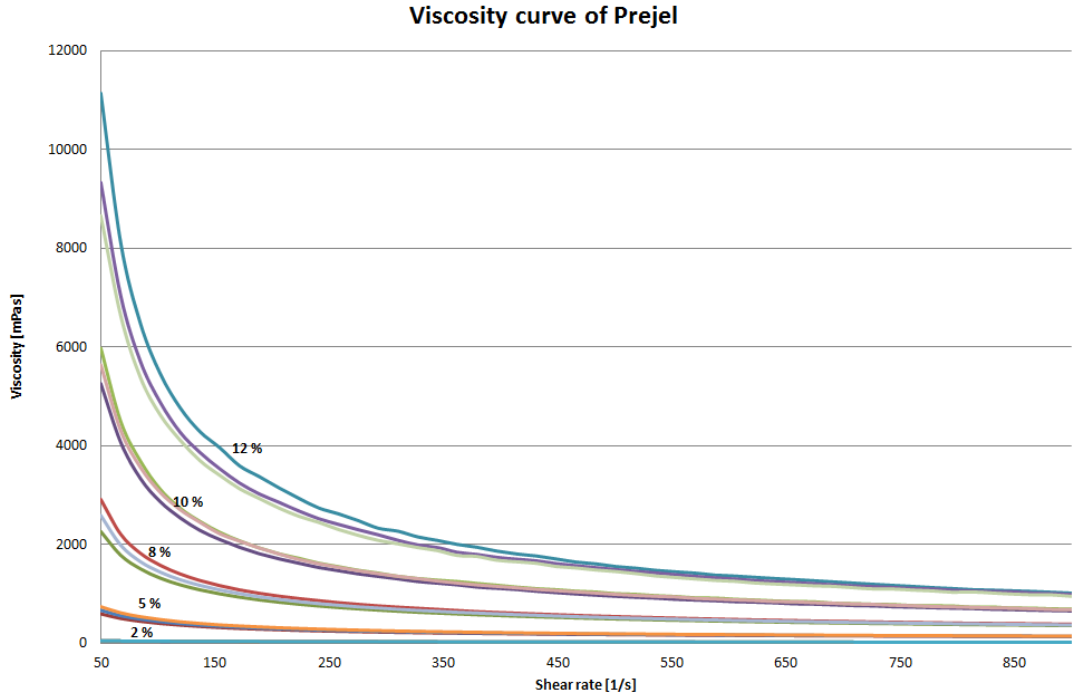

Figure 6. *Viscosity of Prejel as a function of shear rate. Viscosity decreases close to zero as the shear rate increases to its maximum.*

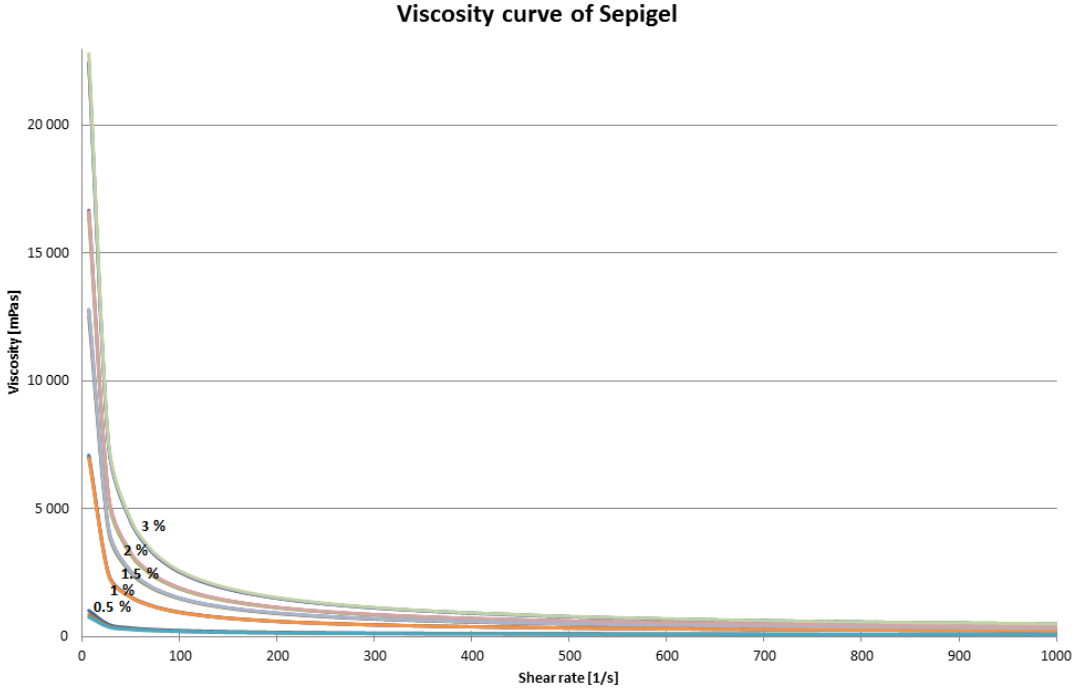

Figure 7. *Viscosity of Sepigel as a function of shear rate. Viscosity decreases close to zero as the shear rate increases to its maximum.*

APPENDIX 3: RAMAN SPECTRA

The Raman spectra of Carbomer 980, Carbopol 974, HPC and Povidone are presented below in Figures 1–4. A Renishaw Ramascope spectrophotometer with LaserPhysics ArIon laser operating at 514 nm at 20 mW was used to measure the Raman spectra. An acquisition time of 10 s and a grating of 2400 l/mm were used for all spectra and the spectra were recorded with a Renishaw WiRE software.

A total of 90 spectra were recorded from Carbomer 980 and Carbopol 974 samples. From HPC and Povidone samples 135 spectra were measured. The spectral range in Carbomer 980, Carbopol 974 and HPC is 350–3500 cm^{-1} and in Povidone the spectra are recorded at 400–3500 cm^{-1}.

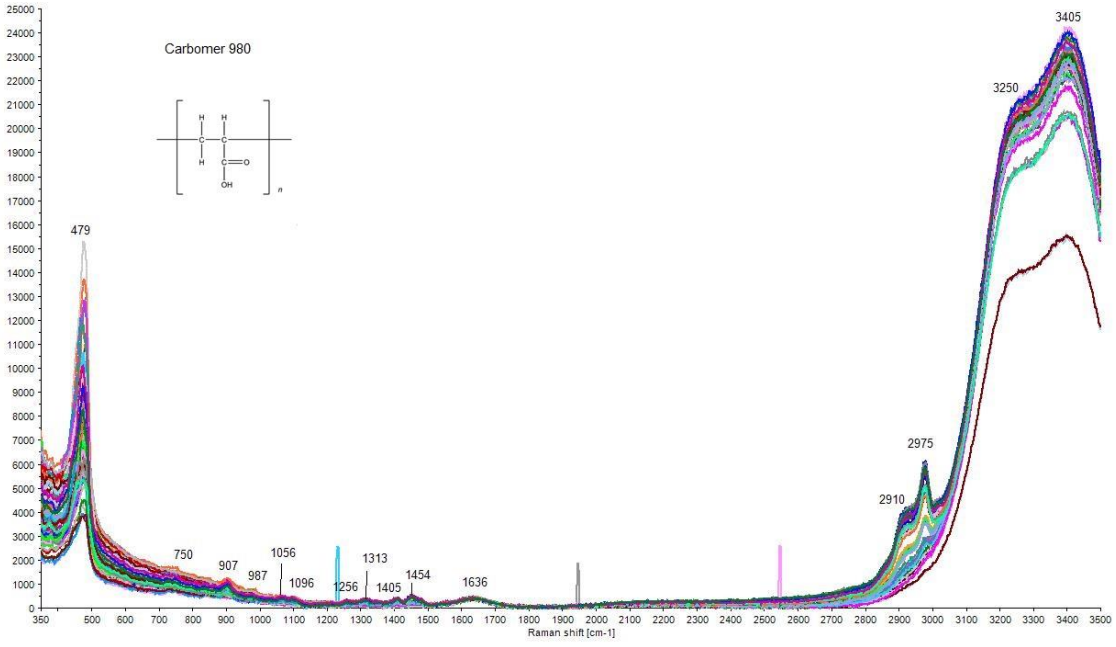

Figure 1. *Raman spectra of the Carbomer 980 samples.*

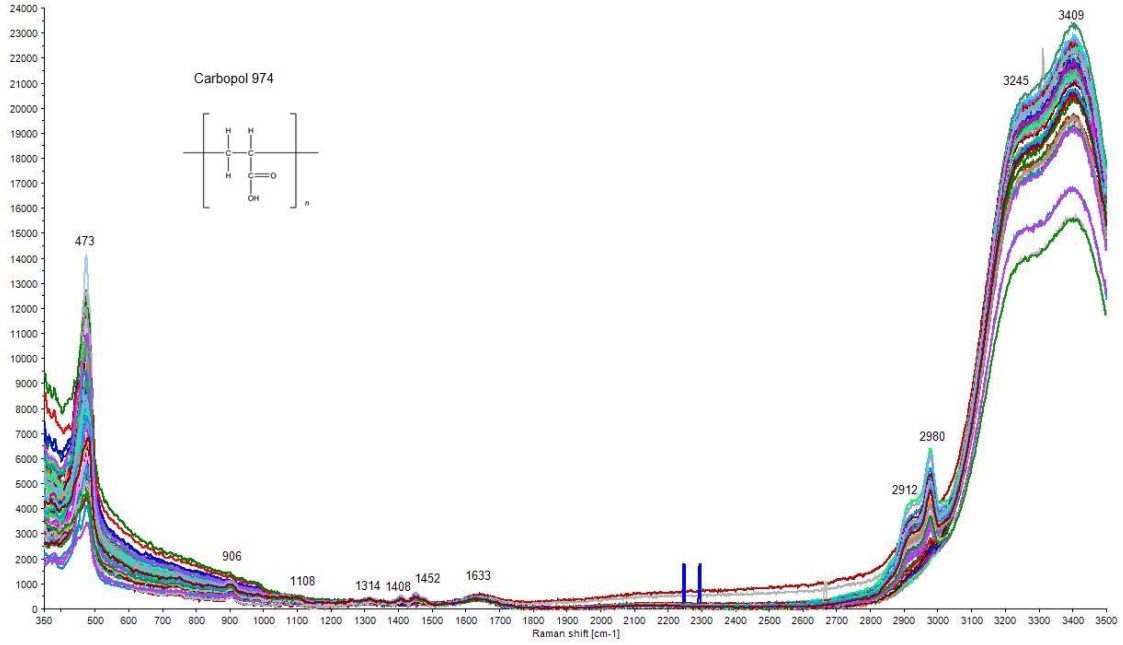

Figure 2. *Raman spectra of the Carbopol 974 samples.*

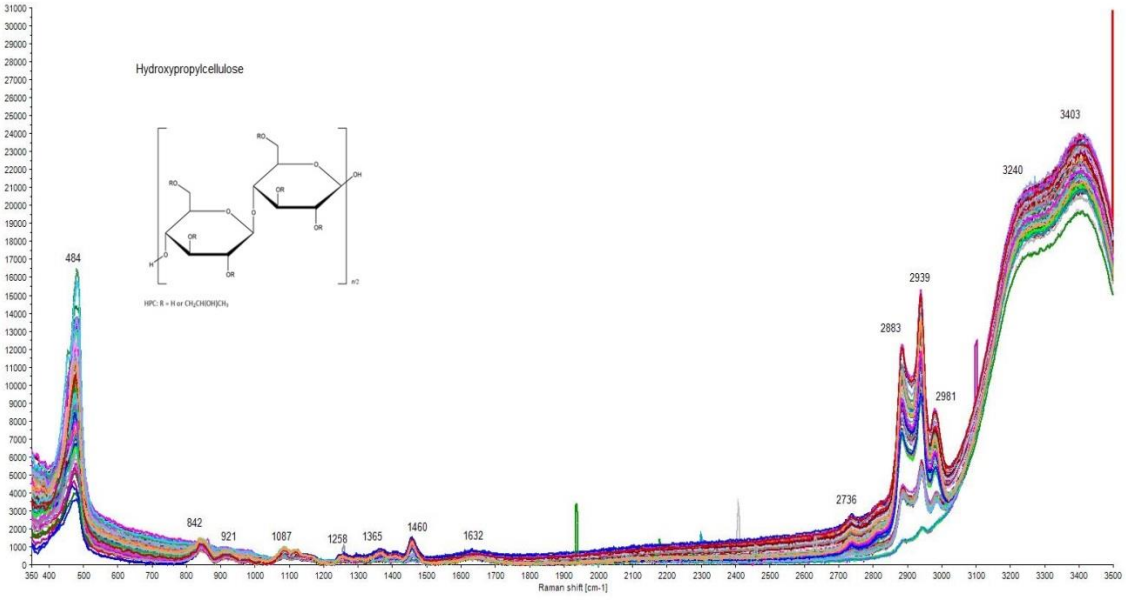

Figure 3. *Raman spectra of the HPC samples.*

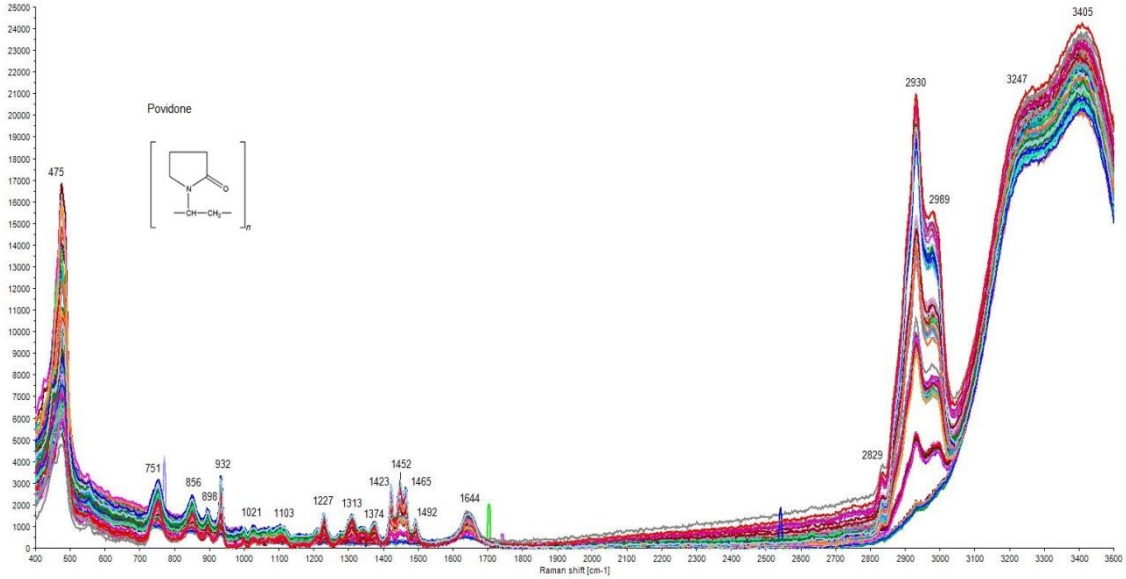

Figure 4. *Raman spectra of the Povidone samples.*